

# Subjective Time Deformation in Intertemporal Choice: A Functional Data Analysis Approach

Fabrizio Maturo\*    Salvador Cruz Rambaud†    Vincenzo Li Calzi‡  
 Andrea Mazzitelli§    Annamaria Porreca¶

## Abstract

Intertemporal choice data are often summarized through scalar discount-rate parameters or fitted by predetermined parametric discount functions. However, when individual choices are observed across several time horizons, relevant information may lie in the shape of the whole discounting trajectory rather than in a single parameter. This paper proposes an applied Functional Data Analysis framework for reconstructing and analyzing implicit subjective-time trajectories from discrete intertemporal equivalence judgments. Monetary equivalence responses collected through a multilingual questionnaire are transformed into individual discount curves, regularized by monotone smoothing, and used to recover normalized implicit subjective-time trajectories. These trajectories are examined through derivative-based summaries, Functional Principal Component Analysis, and clustering on standardized functional principal component scores. The empirical application, based on 107 participants, shows that heterogeneity in intertemporal choice is not fully captured by scalar discount-rate variation. The first two functional principal components explain 97.44% of the variability of the centered trajectories, indicating a low-dimensional functional structure. Functional clustering identifies three stable profiles of temporal deformation. Bootstrap stability analysis and extensive sensitivity checks, involving retained components, clustering algorithms, functional distances, derivative-based semi-metrics, smoothing-basis specifications, and outlier treatment, support the robustness of the main clustering structure. Parametric benchmarks based on exponential, Weber–Fechner, and Stevens specifications show that classical subjective-time models provide accurate fits for many individuals, but do not fully recover the functional clustering structure. The comparison with explicit subjective-time perception measures reveals only partial alignment between implicit trajectories reconstructed from choices and directly reported temporal perception. The results indicate that Functional Data Analysis provides a useful applied statistical framework for representing intertemporal

---

\*Department of Economics, Statistics and Business, Faculty of Technological & Innovation Sciences, Universitas Mercatorum, Rome, Italy. Email: [fabrizio.maturo@unimercatorum.it](mailto:fabrizio.maturo@unimercatorum.it)

†Departamento de Economía y Empresa, Universidad de Almería, Almería, Spain. Email: [scruz@ual.es](mailto:scruz@ual.es)

‡Department of Engineering and Science, Universitas Mercatorum, Rome, Italy. Email: [vincenzo.licalzi@studenti.unimercatorum.it](mailto:vincenzo.licalzi@studenti.unimercatorum.it)

§Department of Economics, Statistics and Business, Faculty of Technological & Innovation Sciences, Universitas Mercatorum, Rome, Italy. Email: [a.mazzitelli@unimercatorum.it](mailto:a.mazzitelli@unimercatorum.it)

¶Department for the Promotion of Human Science and Quality of Life, San Raffaele University, Rome, Italy. Email: [annamaria.porreca@uniroma5.it](mailto:annamaria.porreca@uniroma5.it)

choice heterogeneity as variation in functional shape, complementing scalar discount-rate and parametric subjective-time models.

*Keywords:* intertemporal choice, subjective time, Functional Data Analysis, time distortion, discount curves, clustering.

## 1 Introduction

Intertemporal choices represent a fundamental class of decision-making processes in behavioral economics and the psychology of decision-making. When individuals are required to compare alternatives that differ both in value and in the time at which they are realized, the evaluation of future outcomes depends crucially on the temporal dimension [8]. In this context, time does not constitute a mere external frame of the decision, but directly enters the evaluation process, since an outcome available in the future is generally perceived as less attractive than an outcome available immediately. The classical formulation of this problem is based on the discounted utility model, in which time is treated as an objective and linear variable and the loss of value of future outcomes is represented through an exponential discount function [15]. This framework has long represented the main theoretical reference in the study of intertemporal preferences, due to its formal simplicity and the possibility of summarizing decision behavior through a single discount parameter [3, 8, 15]. However, a large body of empirical evidence has shown that observed behavior often deviates from the predictions of the exponential model [7, 17]. Thus, individuals may exhibit preference reversals, decreasing impatience, the immediacy effect, and other forms of dynamic inconsistency that can not be explained under the assumption of a constant discount rate. From this perspective, anomalies in intertemporal choices should not necessarily be interpreted as simple violations of rationality, but may instead reflect the way individuals perceive and subjectively organize temporal distance. Indeed, the perception of time may not coincide with chronological time. Objectively equal intervals may be experienced as longer or shorter depending on the time horizon considered, the decision context, and certain individual characteristics [2, 7, 17, 19]. A unifying explanation of these behaviors refers to subjective time perception. In effect, individuals do not experience time as a uniform physical dimension, but rather internally transform it in a nonlinear way [19]. Within this perspective, a natural way to formalize this idea consists in maintaining the exponential structure of discounting, but applying it not to chronological time  $t$ , but to a subjective transformation of time [19]. In general terms, the discount function can be expressed as  $F(t) = \exp\{-kg(t)\}$ , where  $k$  represents the discount intensity and  $g(t)$  describes the subjective transformation of time [2]. When  $g(t) = t$ , the classical exponential model is recovered as a special case. When, instead,  $g(t)$  is nonlinear, the discounting dynamics observed with respect to objective time may take forms consistent with compression, expansion, or local variations in temporal sensitivity. In this sense, the central object of analysis is not only the scalar parameter  $k$ , but the temporal transformation itself, which in the empirical part of this study is reconstructed at an individual level as  $\tau_i(t)$  [2, 19]. Despite the theoretical relevance of this perspective, many empirical approaches to subjective time perception rely on predetermined parametric specifications,

such as logarithmic or power transformations. These forms are parsimonious and easily interpretable, but they impose a priori a functional structure that may not be sufficiently flexible to represent the variety of individual profiles. In particular, the subjective time derived from the process of deformation may exhibit regions with different curvature, local changes in speed, and heterogeneous configurations across the entire time horizon. Consequently, an approach based exclusively on a few parameters may conceal a relevant portion of the information contained in individual trajectories. In this context, Functional Data Analysis provides a methodological framework particularly suited to address this problem, as it allows discrete observations to be treated as realizations of a smooth function defined over a continuous domain. Rather than analyzing separately the observed values at individual time horizons, the functional approach considers the entire trajectory as the statistical unit. This makes it possible to reconstruct individual curves, impose constraints consistent with theory, compute derivatives, apply Functional Principal Component Analysis, and identify groups of subjects characterized by similar forms of temporal deformation. In this way, individual variability is not reduced to a single measure of intensity, but instead is studied as heterogeneity in shape along the temporal domain [9, 14, 18]. The present study proposes a framework that integrates intertemporal choice theory and Functional Data Analysis in order to reconstruct and analyze subjective time as a functional object starting from empirical discounting trajectories. The central idea is that the subjective transformation of time,  $\tau_i(t)$ , derived from the equivalence judgments expressed by each individual, can be represented as a continuous function describing how chronological time is internally reorganized into perceived temporal distance. Accordingly,  $\tau_i(t)$  represents subjective time as inferred from choice behavior, and should not be interpreted as a pure psychophysical measure of perceived duration. Rather, it corresponds to an implicit subjective time trajectory reconstructed from intertemporal equivalence judgments. From an empirical perspective, the analysis is based on a multilingual questionnaire administered in Italian, English, and Spanish. Participants provide monetary equivalence judgments across different time horizons, together with explicit measures of subjective time perception, psychometric items related to the perception of time speed, and sociodemographic information. This structure allows for the comparison between an implicit measure of subjective time, derived from intertemporal choices, and an explicit measure obtained through direct evaluation tasks of temporal distance. The comparison between  $\tau_i(t)$  and subjective time perception therefore makes it possible to investigate whether implicit and explicit representations of time capture the same construct or, alternatively, only partially overlapping dimensions. The contribution of this work is therefore twofold. On the one hand, it proposes a flexible methodological procedure to reconstruct individual subjective time without imposing a rigid parametric form. On the other hand, the empirical application shows that intertemporal choices can be interpreted not only through the discount rate, but also through the shape of the function that transforms chronological time into perceived time. This perspective makes it possible to connect more directly intertemporal choice theory, subjective time perception, and functional statistical tools. The remainder of the paper is organized as follows. Section 2 introduces the

relationship between subjective time, temporal distortion, discount function, and the delay function. Section 3 discusses parametric models and measurement approaches for subjective time. Section 4 describes the questionnaire design and data construction. Section 5 presents the functional methodological framework used to reconstruct and analyze individual subjective time trajectories. Section 6 reports the empirical application and results, including functional reconstruction, Functional Principal Component Analysis (FPCA), clustering, comparison between implicit and explicit subjective time, and robustness checks. The paper concludes with a discussion of the main results, the limitations of the analysis, and possible directions for future research.

## 2 Subjective Time and Time Distortion

The mathematical relationship between subjective time, discount function, and intertemporal inconsistency can be described through the concept of temporal distortion. In this framework, the exponential form of discounting is still retained, but it is no longer directly applied to chronological time  $t$ . Instead, the discount function is constructed with respect to a subjective transformation of time, denoted by  $g(t)$ , leading to the following specification

$$F(t) = \exp\{-kg(t)\}, \quad k > 0, \quad (1)$$

where the classical exponential formulation with respect to objective time is recovered when  $g(t) = t$ . When instead  $g(t) \neq t$ , discounting preserves an exponential structure in subjective time, while it may appear non-exponential when expressed in chronological time [2, 3]. In this sense, the concept of time deformation can be formalized through the notion of time distortion, defined as a continuous real-valued function  $g(t)$ , on an interval  $[0, t_0)$ , where  $t_0$  can be  $+\infty$ , satisfying  $g(0) = 0$  and strict monotonicity. The identity function represents the case of no deformation of calendar time, whereas nonlinear specifications of  $g(t)$  describe how chronological time is transformed into subjective time [2]. The specification of  $g(t)$  determines the empirically observed shape of the discount function and makes it possible to interpret certain deviations from the exponential model as the result of an alternative subjective temporal metric. This approach is supported by the literature, which assigns a central role not only to the evaluation of outcomes but also to the perception of the duration separating the present from future outcomes [6]. In particular, the distinction between the *length effect* and the *location effect* shows that the same temporal interval can be evaluated differently depending both on its length and on its position relative to the present [6].

In this light, subjective time becomes an explanatory variable in intertemporal choice. For a given objective duration, waiting may in fact be perceived as longer or shorter by individuals, and the reformulation of preferences with respect to this subjective metric can reduce the hyperbolic curvature of discounting and produce a more regular temporal dynamic [6]. The key point is therefore not to enumerate all possible contexts in which time perception may be altered, but rather to recognize that the temporal metric adopted by the individual can directly influence the evaluation of future outcomes.

An alternative way to formalize intertemporal equivalence relations is provided by the *delay function*  $\Phi_l(s, t)$ , which assigns to a pair  $(s, t)$  the future time  $\Phi_l(s, t)$  such that receiving the reference amount  $l$  at time  $\Phi_l(s, t)$  is equivalent to receiving  $s$  at time  $t$  [1]. This representation allows us to describe the same preferences expressed by a discount function, since a delay function can be derived from a given discount function and, conversely, the structure of intertemporal preferences can be reconstructed from the delay function [1].

The link between intertemporal equivalence and discount trajectories is important because equivalences between amounts and times also constitute the empirical starting point for constructing individual discount trajectories. The instantaneous variation of the discounting process can be described through the instantaneous discount rate,

$$\delta(t) = -\frac{d}{dt} \ln F(t) = -\frac{F'(t)}{F(t)}. \quad (2)$$

In the standard exponential case,  $F(t) = e^{-kt}$ , a constant value  $\delta(t) = k$  is obtained. If instead discounting is expressed in terms of subjective time,  $F(t) = e^{-kg(t)}$ , then

$$\delta(t) = kg'(t), \quad (3)$$

so that the evolution of impatience depends on the rate at which subjective time increases relative to chronological time [1]. In this formulation,  $g'(t)$  describes how an infinitesimal increase in objective time is converted into a change in perceived time. The nonlinearity of  $g(t)$  is therefore not merely a mathematical detail, but becomes the mechanism through which subjective duration perception modifies the shape of the discount function.

The same idea can be expressed when using the delay function through the instantaneous rate of change

$$v(l, s, t) = \frac{\delta(\Phi_l(s, t))}{\delta(t)}. \quad (4)$$

When  $F(t) = \exp\{-kg(t)\}$ , this parameter can be written as

$$v(l, s, t) = \frac{g'(\Phi_l(s, t))}{g'(t)}. \quad (5)$$

This relationship shows that the variation in impatience can be interpreted as the ratio between two velocities of subjective time, evaluated respectively at  $t$  and at the equivalent time  $\Phi_l(s, t)$  [1]. Intertemporal inconsistency can thus be interpreted as a variation in the speed at which subjective time evolves along the temporal domain.

The relationship between temporal distortion and decreasing impatience can be understood as a condition linking the shape of the discount function to the curvature of the subjective time transformation [13]. When discounting is expressed in exponential form with respect to subjective time, as in (1), decreasing impatience arises when the logarithm of the discount function is convex. This is equivalent to requiring that the subjective time function  $g(t)$  be concave [13]. Intuitively, if  $g(t)$  is concave, each increase in objective time translates into a progressively smaller increase in perceived time, so that the impact of waiting decreases as the time horizon increases.

This relationship can be represented through the so-called Prelec’s index

$$P(t) = -\frac{d}{dt} \ln \delta(t), \quad (6)$$

which describes the local variation of impatience over time [1, 13]. Since, in the model  $F(t) = \exp\{-kg(t)\}$ , one has  $\delta(t) = kg'(t)$ , the form of  $g(t)$  directly determines the dynamics of impatience. A concave function  $g(t)$  therefore implies a progressive reduction in the speed of subjective time, providing a formal explanation of the link between perceived time compression, decreasing impatience, and non-exponential discounting.

This result connects to the psychophysical literature on time perception, a field that analyzes the relationship between physical stimuli and perception, showing how objective time  $t$  can be transformed into perceived duration  $g(t)$  through nonlinear laws [16]. Classical formulations, such as the Weber–Fechner law and Stevens’ law, precisely describe this mapping from real time to subjective time [16]. They therefore constitute the natural starting point for discussing parametric models of subjective time, their interpretative advantages, and their limitations in capturing individual heterogeneity in temporal distortion.

### 3 Parametric Models and Measurement of Subjective Time

Research on subjective time perception has proposed several mathematical representations aimed at describing how chronological time is transformed into perceived time. One contribution in this direction introduces a quantitative model of subjective temporal compression in which the subjective unit  $U_s$  decreases progressively as lived temporal experience increases [4]. In general form, this relationship is defined as

$$U_s = U_s(a, t) = \frac{U_o}{t^a}, \quad 0 \leq a \leq 1, \quad (7)$$

where  $U_o$  denotes the objective time unit, whereas the parameter  $a$  governs the intensity of subjective compression [4]. Considering a time interval  $[s, t]$ , the variation in subjective time can be expressed as

$$g(s, t) = \int_s^t x^{-a} dx = \begin{cases} \log\left(\frac{t}{s}\right), & \text{if } a = 1, \\ \frac{t^{1-a} - s^{1-a}}{1-a}, & \text{if } a \neq 1. \end{cases} \quad (8)$$

This formulation shows that subjective time compression may lead, depending on the value of the parameter  $a$ , either to a logarithmic form or to a power-law type representation. In the case  $a = 1$ , perceived time grows according to a logarithmic structure. However, when  $a < 1$ , by setting  $\gamma = 1 - a > 0$ , a representation of the form

$$g(t) = \frac{1}{\gamma} t^\gamma, \quad (9)$$

is obtained, which exhibits a formal parallelism with Stevens’ law and describes an increasing and concave function when  $0 < \gamma < 1$  [4]. The central aspect of this model does not lie

so much in its broader sociopsychological interpretation, but rather in its ability to represent time perception through nonlinear mathematical transformations capable of capturing compression and diminishing growth of subjective time.

The literature identifies two particularly important formulations for describing the link between subjective time and discounting, namely a logarithmic transformation of perceived duration and a power-law transformation. According to the Weber–Fechner’s law, perceived duration grows logarithmically with respect to the objective time and, in the context of intertemporal choice, this transformation can be expressed as

$$g_1(t) := \alpha \ln(1 + \beta t), \quad \alpha > 0, \beta > 0, \quad (10)$$

where  $\alpha$  represents a scaling parameter of subjective duration and  $\beta$  controls the initial slope of the transformation [16]. The function is increasing but characterized by a progressively decreasing slope, suggesting that additional increments in time produce increasingly weaker subjective effects. This property is particularly relevant in intertemporal decisions, as it allows decreasing impatience to be interpreted as a consequence of the concave temporal transformation. The second model, Stevens’ law, instead proposes a power-law relationship between objective time and perceived time, which can be written as

$$g_2(t) = \alpha t^\beta, \quad \alpha > 0, \beta > 0, \quad (11)$$

where  $\alpha$  determines the overall scale of the subjective measure, whereas the exponent  $\beta$  controls the curvature of the transformation [16]. When  $0 < \beta < 1$ , the function is increasing and concave, so that each additional time interval yields progressively smaller subjective increments. When  $\beta = 1$ , the transformation is linear. When  $\beta > 1$ , the function becomes convex and time increments produce increasing subjective effects [16]. These two formulations therefore constitute fundamental parametric tools for modelling the transformation of chronological time into subjective time.

Subjective time measurement can also be described through the speed at which perceived duration changes relative to real time [12]. In this direction, the so-called Rate of Subjective Time is introduced, defined as

$$\text{RST} = \frac{dT}{dt}, \quad (12)$$

where  $T$  denotes perceived time and  $t$  real time. This quantity can be interpreted as the derivative of the subjective time transformation,

$$\text{RST} = g'(t). \quad (13)$$

This relationship is particularly relevant because it directly links the psychological measurement of subjective time speed to the mathematical structure of the function  $g(t)$ . If  $g'(t)$  decreases as  $t$  increases, then  $g(t)$  is concave and the subjective time transformation describes a progressive compression of perceived duration. In this sense, the speed of subjective time constitutes a natural bridge between the psychological measurement, the curvature of the temporal function, and the dynamics of impatience.

In the existing literature, an important contribution to the measurement of subjective time in intertemporal decisions has been obtained through an approach in which participants are asked to represent different temporal horizons on a continuous line connecting the present and the future. The obtained positions are then converted into units of perceived time, allowing the relationship between real time and subjective time to be analyzed [19]. The results show that, as time increases, human perception does not grow proportionally but much more slowly, following a nonlinear and concave curve [19]. This implies that when discounting is measured with respect to chronological time, it tends to take a hyperbolic form, whereas when it is recalculated in terms of perceived time the dynamics appear more regular and closer to an exponential form [19]. These findings suggest that some inconsistencies in intertemporal choices may arise from the psychological compression of future time.

An interpretation in the literature proposes that hyperbolic discounting can be explained by distinguishing between chronological time and subjective time [5]. When moving from a calendar-based representation of time to a perception-based representation, the apparently hyperbolic pattern observed as a function of  $t$  can become a more regular exponential structure when expressed as a function of  $g(t)$  [5]. Two aspects are particularly important: diminishing sensitivity, according to which subjective time increases less than proportionally as the temporal horizon expands, and time contraction, which describes the overall extent to which future horizons are perceived as shorter or longer than calendar time [5]. For this reason, time perception can be described through nonlinear transformations such as logarithmic or power laws, and discount rates may appear decreasing with respect to objective time while becoming more stable when expressed in the subjective metric  $g(t)$  [5].

From a mathematical perspective, when the Weber–Fechner transformation, which describes the nonlinear growth of time perception, is inserted into an exponential discount function defined over subjective time, the resulting behavior observed in real time becomes hyperbolic. In particular, by setting  $g(t) = \alpha \ln(1 + \beta t)$  in the exponential function (1), a function depending on real time is obtained that takes a hyperbolic form [2, 16]. The resulting expression is

$$F(t) = (1 + \beta t)^{-k\alpha}. \quad (14)$$

In the special case  $k\alpha = 1$ , this expression coincides with the classical hyperbolic form,

$$F(t) = \frac{1}{1 + \beta t}. \quad (15)$$

This result clearly shows that non-exponential discounting in real time can arise from an exponential structure applied to a subjective time scale that does not grow linearly [2, 16]. Representations based on logarithmic, power-law, and hyperbolic forms therefore constitute useful and interpretable theoretical tools for describing subjective time, but they require the prior assumption of a specific functional form. This becomes a limitation when the aim is not only to describe an average tendency, but also to capture individual heterogeneity in temporal distortion. Subjective time transformations may exhibit local changes in curvature, regions of stronger compression or dilation, and individual profiles that are not fully reducible to a single parametric family. For this reason, although parametric models represent an

essential starting point, they need to be extended towards a more flexible representation when subjective time is treated as a continuous individual trajectory. This motivates the use of the Functional Data Analysis, which allows  $\tau_i(t)$  to be reconstructed as an individual functional object and analyzed in terms of shape, derivatives, dimensional structure, and recurrent patterns of temporal deformation.

## 4 Questionnaire Design and Data Construction

The empirical structure of the questionnaire is presented prior to the introduction of the analytical procedure, since the objects used in the methodology are directly derived from the design of the data collection instrument. This choice makes it possible to define the empirical variables used for the construction of discount curves, the reconstruction of subjective time trajectories, and the comparison between implicit and explicit measures of temporal perception. Data collection was carried out through a multilingual online questionnaire, available in Italian, English, and Spanish, designed to jointly investigate intertemporal preferences, the subjective perception of time, and a set of individual characteristics potentially associated with decision-making processes. The questionnaire was presented as a university study aimed at analyzing subjective time perception and the way individuals evaluate rewards or payments occurring in the future, explicitly clarifying to participants that there are no correct or incorrect answers and that responses should reflect only their personal perception and experience. The questionnaire design integrates both implicit and explicit measures of subjective time. The implicit component is obtained through monetary equivalence judgments, in which each participant indicates which amount received immediately they consider equivalent, in terms of subjective value, to a fixed future reward of 100 euros. This procedure allows for the construction, for each individual, of discrete observations of the discount function at different time horizons. The considered horizons are thirteen in total and span from 7 days to 5 years, including 7, 14, and 21 days, 1, 2, 3, 4, 6, and 9 months, and 1, 2, 3, and 5 years. These responses constitute the starting point for the construction of individual discount trajectories and, subsequently, of the subjective time functions  $\tau_i(t)$ , according to the methodological procedure described in the following section. The explicit component of time perception is instead elicited through the STP task, in which, for the same time horizons used in the equivalence judgments, each participant subjectively places each horizon along a line ranging from the present to the future. This procedure follows the subjective time estimation approach based on positioning along a temporal continuum [19]. The STP responses are normalized by using, for each participant, the cursor position associated with the 7-day horizon as an individual calibration anchor. The resulting normalized value expresses perceived temporal distance in subjective months, taking the 7-day horizon as the reference unit, equal to  $7/30.42 \approx 0.23$  months. In this way, the questionnaire allows for the comparison of an implicit measure of subjective time, reconstructed from intertemporal choices, with an explicit measure based on stated evaluations of perceived temporal distance. The questionnaire also includes psychometric measures and individual

covariates used to describe heterogeneity in functional profiles. In particular, a Temporal Sense Scale is collected, in which participants rate the perceived speed of time on a scale from 1 to 7, ranging from “very slowly” to “very quickly”, with reference to different time windows. Additional information is collected on socio-demographic characteristics, financial literacy variables, perceived health status, physical activity, chronic physical or psychological conditions, sleep, caffeine, alcohol and tobacco consumption, use of supplements, gambling behavior, future orientation, present focus, and perceived stress. These variables do not constitute the core of the functional analysis, but allow for characterizing participants and for assessing, in subsequent analyses, potential descriptive associations between the shapes of the subjective time function and relevant individual differences. Since the questionnaire was administered in three languages, categorical variables and some textual responses were harmonized into a common coding scheme prior to the analyses. Responses concerning gender, educational level, employment status, income, and other covariates were recoded into homogeneous categories. The items of the Temporal Sense Scale were recoded on a numerical scale from 1 to 7 and subsequently used to construct a synthetic index of perceived time speed. This harmonization step is necessary to ensure comparability of responses collected across the different language versions of the questionnaire and to construct a single coherent dataset consistent with the subsequent functional analyses. The questionnaire was completed by 113 participants. The final analytical sample used for FDA, FPCA, clustering, and robustness analysis consists of  $N = 107$ , after excluding one participant with missing equivalence responses and five participants identified as functional outliers based on the second derivative of  $\tau_i(t)$ . Descriptive characteristics of the final analytical sample are reported in Table 1.

## 5 Functional Methodological Framework

Functional Data Analysis (FDA) represents an approach designed to analyze phenomena observed over a continuous domain, in which the relevant information does not lie solely in the individual observed values, but above all in the overall shape of the function describing them. The fundamental idea consists in considering a sequence of scalar observations as the discrete manifestation of an underlying continuous function that is not directly observed. This makes it possible to treat each statistical unit as a single functional object rather than as a vector of separate measurements [14]. Consequently, the analysis is not limited to individual observed points, but also considers the overall properties of the curves and their local variations, providing a more natural description of dynamic phenomena. This type of approach is particularly effective in the study of data characterized by high structural complexity, high dimensionality, or patterns of variation that cannot be adequately described through traditional statistical techniques. Functional representation makes it possible to combine regularization techniques, the use of functional bases, derivative analysis, curvature analysis, and dimensionality reduction procedures, thereby mitigating the effects of the *curse of dimensionality* [10]. In the study of intertemporal choice, these characteristics play an

Table 1: Descriptive characteristics of the final analytical sample ( $N = 107$ ), after exclusion of incomplete equivalence responses and functional outliers.

<b>Variable</b>	<b>Category</b>	<i>N</i>	%
Gender	Female	57	53.3
	Male	50	46.7
Education	Upper secondary	35	32.7
	Bachelor	17	15.9
	Master's degree	43	40.2
	PhD	8	7.5
	Other/Lower	4	3.7
Employment	Full-time	40	37.4
	Part-time	23	21.5
	Student	17	15.9
	Self-employed	13	12.1
	Other/Retired	14	13.1
Income (EUR/year)	< 10,000	23	21.5
	10,000–20,000	20	18.7
	20,001–40,000	30	28
	40,001–60,000	9	8.4
	$\geq 60,001$	4	3.7
	Prefer not to say	21	19.6
Age: mean = 39, SD = 12.4, range [18–73]			
TSS <sub>core</sub> : mean = 4.94, SD = 1.15			
Financial literacy: mean = 1.82, SD = 0.89 (range 0–3)			

important role because discount functions and subjective transformations of time may exhibit structures that are not fully compatible with a parametrically specified functional form. Although parametric models are characterized by interpretability and parsimony, they still require the structure of the discount function or the subjective temporal transformation to be specified in advance. This assumption may become restrictive when the observed behavior displays individual differences, local variations, and heterogeneous temporal profiles along the considered horizon [9]. FDA makes it possible to represent discount trajectories and subjective time functions as continuous curves defined over the temporal domain, providing a more flexible description than a purely parametric approach [18]. In the present work, this framework is employed to reconstruct subjective time through intertemporal equivalence judgments collected by questionnaire. For each participant, these judgments generate discrete observations of the discount function at different temporal horizons. However, since temporal perception and the evaluation of future outcomes evolve along a continuum, treating such values as separate observations would risk overlooking the overall dynamics of the phenomenon. FDA makes it possible to interpret them as points belonging to an underlying functional trajectory and to reconstruct continuous curves that can be analyzed over the entire temporal domain [14]. The individual subjective function can be represented through a linear combination of functional bases in the form

$$\tau_i(t) \approx \sum_{b=1}^B c_{ib} \phi_b(t), \quad (16)$$

where  $\phi_b(t)$  denotes the basis functions,  $c_{ib}$  the coefficients specific to individual  $i$ , and  $B$  the number of considered bases, thus determining the level of flexibility of the final representation. In this context, the reconstruction of subjective curves is developed while taking into account the theoretical properties of temporal perception. In particular, since subjective time is assumed to increase together with objective time, the monotonicity constraint is directly incorporated into the estimation procedure through Shape Constrained Additive Models (SCAM). In this way, the resulting curves remain consistent with the theoretical interpretation attributed to subjective time and can be studied in an interpretable manner over the entire temporal domain. Through this framework, discretely observed and potentially noisy data can be reinterpreted as a continuous function. Consequently, the focus is not limited to the intensity with which an individual discounts the future, but also concerns the shape assumed by the function  $\tau_i(t)$ , which describes the process through which calendar time is transformed into perceived time. The central methodological element lies precisely in the fact that the subjective deformation of time is not defined through a parametric law fixed a priori, but is instead reconstructed as an individual functional trajectory, making it subsequently possible to analyze its overall shape, local variations, dimensional structure, and the presence of recurring configurations.

## 5.1 From Equivalence Judgments to Subjective Time Functions

The empirical reconstruction of subjective time starts from the intertemporal equivalence judgments collected through the questionnaire. For each participant  $i$  and for each temporal

horizon  $t$ , the observed quantity is the immediate amount  $A_{0,i}(t)$  that the subject considers equivalent to receiving a fixed future reward equal to  $A_f = 100$ . This value represents the amount available immediately that, from the participant's subjective perspective, compensates for the waiting time required to obtain the future reward. The observed judgment is then normalized with respect to the future amount and represented as a point of the individual discount function,

$$f_i(t) = \frac{A_{0,i}(t)}{A_f}, \quad (17)$$

with  $A_f = 100$  euros in the empirical design considered. In this way, each response is interpreted as the proportion of the future reward that the participant would be willing to accept immediately. Lower values of  $f_i(t)$  indicate a stronger devaluation of the future, whereas values close to one indicate a smaller subjective reduction in the value of the delayed reward [18]. The observed values of  $f_i(t)$  are available only at a finite number of temporal horizons and therefore constitute a discrete, and potentially noisy, representation of the individual discounting process.

However, since intertemporal decisions naturally evolve along a continuous temporal axis, treating these values as isolated observations would not allow an adequate description of the overall trajectory dynamics. For this reason, before reconstructing subjective time, the data are subjected to a smoothing phase under a monotone decreasing constraint. This constraint reflects the theoretical principle according to which the value assigned to a future reward should not increase as the delay becomes longer [18]. In practical terms, all values violating the theoretical domain of the discount function, namely  $f_i(t) \leq 0$  or  $f_i(t) > 1$ , are treated as missing values, whereas the initial point  $t = 0$  is added as a theoretical constraint imposing  $f_i(0) = 1$ . Subsequently, for each individual, a smooth function  $\hat{f}_i(t)$  is estimated over a common temporal grid, thereby obtaining a continuous and coherent representation of the individual discount trajectory. The construction of the subjective time function is based on the assumption that discounting behavior can be described through an exponential structure applied not directly to chronological time, but to a subjective transformation of time. In this framework, the discount function takes the form

$$f_i(t) = \exp\{-k_i\tau_i(t)\}, \quad (18)$$

where  $k_i$  denotes the individual parameter governing the intensity of discounting and  $\tau_i(t)$  represents the subjective time function associated with individual  $i$ . When  $\tau_i(t) = t$ , the classical exponential model based on objective time is obtained, whereas differences between the two quantities indicate a subjective distortion of temporal perception. The nonlinearity of  $\tau_i(t)$  therefore describes not only a different intensity of discounting, but also a different subjective organization of temporal distance. Applying the natural logarithm to the previous relationship yields

$$-\log f_i(t) = k_i\tau_i(t). \quad (19)$$

This formulation makes it possible to reconstruct subjective temporal perception starting from the observed discount function. Once the parameter  $k_i$ , used as an individual reference

for the intensity of discounting, has been estimated, the function  $\tau_i(t)$  can be derived from the estimated discount function. The parameter  $k_i$  is estimated through a regression without intercept between  $-\log \widehat{f}_i(t)$  and chronological time  $t$ , thereby constructing for each subject a reference consistent with the exponential model defined on objective time. After this initial estimation, a first reconstruction of subjective time is defined as

$$\tau_{\text{raw},i}(t) = \frac{-\log \widehat{f}_i(t)}{k_i}. \quad (20)$$

The resulting curve is then regularized through a monotone increasing smoothing procedure implemented using Shape Constrained Additive Models (SCAM), imposing that subjective time cannot decrease as chronological time increases. After monotone refitting, each trajectory is normalized so that  $\tau_i(0) = 0$ . This step fixes a common origin for subjective time and improves comparability across individuals. Since this normalization is applied after the recovery of  $\tau_{\text{raw},i}(t)$ , the resulting function is interpreted as a normalized implicit subjective time trajectory conditional on the estimated individual discounting scale  $k_i$ . The final result is a continuous and monotone individual function  $\tau_i(t)$ , defined over the entire observed temporal domain.

## 5.2 Identification and Normalization of Subjective Time Functions

An important aspect of the procedure concerns the interpretation of the parameter  $k_i$  and the function  $\tau_i(t)$ . In the model

$$f_i(t) = \exp\{-k_i\tau_i(t)\}, \quad (21)$$

the discount function is determined both by the parameter  $k_i$ , which represents the intensity of discounting applied to future outcomes, and by the function  $\tau_i(t)$ , which represents the time perceived by the subject. These two components do not operate separately, but enter the formula jointly through their product. For this reason, they cannot be considered completely independent quantities in an absolute sense. In other words, two individuals may differ not only because one discounts more strongly than the other, but also because they transform time differently across the temporal horizon. For this reason,  $k_i$  is estimated first and then used as a reference parameter, namely as a preliminary measure allowing the definition of an individual discounting scale. Once this scale has been fixed, it becomes possible to reconstruct the function  $\tau_i(t)$  and study the shape of the subjective temporal trajectory. The main objective is therefore not to perfectly separate what depends on discounting from what depends on temporal perception, but rather to obtain an interpretable function that allows the analysis of how chronological time is subjectively transformed by different individuals. The primary interest concerns the shape of the function  $\tau_i(t)$ , namely the way in which perceived time grows, slows down, accelerates, or changes structure across different temporal horizons. For this reason, in the present framework  $\tau_i(t)$  should be interpreted as a normalized subjective time trajectory, conditional on the individual discounting scale fixed by  $k_i$ , rather than as an absolute and uniquely identified separation between discount intensity and time perception. A strong assumption of the proposed reconstruction is

that deviations from exponential discounting in chronological time are represented through the function  $\tau_i(t)$ . Consequently, the recovered trajectory may absorb not only temporal perception in a strict psychophysical sense, but also other behavioral components affecting equivalence judgments, such as response noise, uncertainty, magnitude effects, or contextual features of the task. For this reason,  $\tau_i(t)$  is interpreted as an implicit subjective time trajectory reconstructed from choices, rather than as a direct psychophysical measure of perceived duration.

### 5.3 Derivative-Based Analysis of Subjective Time Trajectories

Once the functions  $\tau_i(t)$  have been obtained, their analysis is not limited to the global shape of the trajectory, but also concerns local variations along the temporal domain. In particular, the first derivative

$$\tau_i'(t) \tag{22}$$

describes the local speed of subjective time, namely the way in which an increase in chronological time translates into an increase in perceived temporal distance. Higher values of  $\tau_i'(t)$  indicate regions of the domain in which subjective time expands more rapidly, whereas lower values indicate regions in which the growth of perceived time is slower. The second derivative

$$\tau_i''(t) \tag{23}$$

instead describes the acceleration of the function and therefore the change in the speed of subjective time across temporal horizons. It makes it possible to interpret variations in subjective sensitivity to delays. Negative values of  $\tau_i''(t)$  reflect a progressive reduction in temporal sensitivity, consistent with a compression of perceived time and with forms of decreasing impatience. Positive values instead indicate an increase in sensitivity to delays and a possible local expansion of perceived temporal distance. In this way, derivatives make it possible to move from a simple reconstruction of the subjective curve to a dynamic interpretation of temporal deformation, thereby preparing the subsequent functional analyzes based on FPCA and clustering.

### 5.4 Functional Principal Component Analysis of Subjective Time Trajectories

After reconstructing the individual subjective time functions  $\tau_i(t)$ , the application of Functional Principal Component Analysis to the centered trajectories makes it possible to study the main sources of individual variability in time perception. To analyze individual differences in subjective time trajectories, the functions  $\tau_i(t)$  are first compared with respect to an average profile constructed over the entire sample. To this end, the sample mean function is subtracted from each individual curve, obtaining

$$\tau_i^c(t) = \tau_i(t) - \bar{\tau}(t). \tag{24}$$

This operation makes it possible to isolate individual variability from the average structure shared across the sample. The analysis therefore focuses on differences in the shape of

the trajectories, namely on the way each individual modifies the perception of temporal distance relative to the average profile observed over the temporal domain. Subsequently, the centered functions  $\tau_i^c(t)$  are represented through a linear combination of functional principal components,

$$\tau_i^c(t) \approx \sum_{m=1}^M \xi_{im} \psi_m(t), \quad (25)$$

where  $\psi_m(t)$  denotes the  $m$ -th functional principal component, whereas  $\xi_{im}$  represents the score of individual  $i$  associated with that component. The components  $\psi_m(t)$  make it possible to identify the dominant structures of functional variability, whereas the scores  $\xi_{im}$  summarize individual behavior along these main directions. In this sense, FPCA allows the variability of subjective trajectories to be summarized through a reduced number of dimensions while preserving the essential characteristics of the observed functions [10, 14]. FPCA makes it possible to study the variability of subjective trajectories while maintaining attention on the overall shape of the functions  $\tau_i(t)$ . Through this analysis, it becomes possible to distinguish variations that affect the global structure of subjective temporal deformation from more localized variations emerging only within specific regions of the temporal domain. The scores associated with the functional principal components allow each functional trajectory to be transformed into a reduced set of synthetic coordinates while still preserving the essential information related to the shape of the curve. This makes it possible to reduce the complexity of the observed functions while maintaining the fundamental characteristics of their structure and therefore allows individual heterogeneity to be analyzed without reducing the entire function to a single scalar parameter. The scores obtained from FPCA can also be used as a basis for identifying groups of individuals characterized by similar profiles of subjective time. In this sense, FPCA is not only a descriptive tool, but also represents an intermediate methodological step between the reconstruction of the functions  $\tau_i(t)$  and the subsequent analyzes based on functional clustering. The main interest does not consist solely in measuring the intensity of discounting, but in describing the functional structure of subjective time perception and the main configurations of heterogeneity across individuals.

## 5.5 Functional Clustering of Subjective Time Profiles

After estimating the individual subjective time functions and describing their variability through Functional Principal Component Analysis, the analysis can be oriented toward the identification of recurring patterns of temporal deformation. The aim of functional clustering is to detect groups sharing similar structures of the function  $\tau_i(t)$ , rather than classifying individuals on the basis of a single quantitative discounting index. To enable such a comparison, clustering is performed on the scores obtained from FPCA, thereby relying on a compact but informative representation of the subjective trajectories. This choice allows the analysis to focus on the main directions of functional variability identified by FPCA, avoiding that classification depends solely on pointwise observations or isolated differences at specific time horizons [10, 14]. A preliminary step before clustering consists in standardizing the FPCA scores, since different principal components explain different proportions

of variability and, without this adjustment, the component with the largest variance would dominate the distance metric used for grouping. Standardization therefore ensures that scores contribute comparably to the construction of clusters and prevents the group structure from being driven almost exclusively by the dominant component. Clustering is then performed using a  $k$ -means algorithm applied to the standardized FPCA scores, employing multiple random initializations in order to reduce dependence of the solution on specific starting configurations. The number of clusters is selected using the average silhouette criterion, an index that jointly evaluates within-group cohesion and between-group separation. The optimal solution is the one that maximizes this value, as it achieves the best trade-off between cluster compactness and separation across groups. This approach is particularly suitable in functional clustering settings, especially when curves are represented through functional scores or dimension-reduction bases [10, 11]. The stability of the clustering solution is further assessed through a bootstrap procedure based on repeated resampling of the dataset and comparison between the resulting partitions and the original one. Similarity across cluster configurations is measured using the Jaccard index, which quantifies the degree of overlap between groups and thus their robustness to data perturbations. High values of the index indicate stable clusters, whereas lower values suggest a more fragile structure that is sensitive to the specific sample. In this way, the analysis does not rely solely on selecting an optimal solution according to the silhouette criterion, but also incorporates an assessment of the empirical robustness of the obtained partitions. Since clustering is carried out on functions  $\tau_i(t)$  centered with respect to the sample mean, the key point is to examine how individual trajectories deviate from the sample average. For this reason, clusters should not be interpreted as distinct “laws” of subjective time. Instead, they represent an exploratory partition of the individual functions that captures recurring patterns of temporal deformation. Their role is to highlight functional heterogeneity, not to replace the idea of an underlying common structure. In this context, positive values of the cluster mean function indicate time intervals in which the trajectories in that group lie, on average, above the sample mean, while negative values indicate positions below it, making the classification mainly dependent on when and how deviations from the mean profile occur. To interpret the obtained groups, functional centroids are computed, defined as the pointwise average of the centered curves belonging to each cluster. Denoting with  $C_g$  the  $g$ -th group and with  $n_g$  the number of subjects in it, the functional centroid can be expressed as

$$\bar{\tau}_g^c(t) = \frac{1}{n_g} \sum_{i \in C_g} \tau_i^c(t), \quad (26)$$

where

$$\tau_i^c(t) = \tau_i(t) - \bar{\tau}(t) \quad (27)$$

represents the centered subjective trajectory of individual  $i$ . This representation allows the average shape of temporal deformation within each group to be described and enables comparison of clusters across the entire time domain. Overall, functional clustering represents the step that moves from the variability of individual trajectories  $\tau_i(t)$  to the identification

of recurring configurations of subjective time deformation. The aim is not to obtain a purely descriptive classification, but to identify interpretable functional profiles capable of capturing differences in shape, curvature, and temporal dynamics of subjective trajectories. In this sense, clusters are understood as patterns of deviation from the sample mean rather than as simple groupings based on discount intensity.

## 5.6 Comparison between Implicit and Explicit Subjective Time Measures

The final part of the analysis considers two distinct ways of measuring subjective time. The first is an implicit measure, reconstructed from intertemporal equivalence judgments and represented by the function  $\tau_i(t)$ . This measure is derived from choice behavior, as it is obtained from the individual discount function and describes how chronological time is transformed in the subjective evaluation of future rewards. The second is an explicit measure obtained through the task known as STP, Subjective Time Perception, in which each participant places different temporal horizons along a continuum ranging from the present to the future, following a procedure of subjective estimation of temporal duration [19]. The two measures therefore do not originate from the same type of response. The function  $\tau_i(t)$  is indirectly obtained from monetary equivalence judgments, whereas the STP measure is based on a direct assessment of perceived temporal distance. Since the STP task and the reconstructed  $\tau_i(t)$  are expressed on different scales, the comparison focuses on standardized shapes rather than absolute levels. STP profiles are therefore standardized within individuals before cluster-level comparison. The joint availability of an implicit and an explicit measure allows an examination of whether they refer to the same latent process or instead capture different dimensions of subjective time perception. This comparison should not be interpreted as a strict validation in which one measure is considered correct and the other incorrect. The aim is to understand whether subjective time reconstructed from choice behavior and subjective time directly reported exhibit similar structures or only partial overlap. The comparison plays mainly an interpretative and exploratory role, as it allows the investigation of whether the functional structures reconstructed through  $\tau_i(t)$  are also reflected in the average STP trajectories of subjects belonging to the same groups. The comparative analysis is developed along two distinct levels. The first concerns the structure of the subjective temporal trajectories. In this case, the functional centroids of the clusters obtained from the centered functions  $\tau_i^c(t)$  are compared with the corresponding mean STP profiles computed within the same clusters. Since the two measures are expressed on different scales, a direct comparison of absolute values would not be particularly informative. For this reason, the analysis focuses on the similarity in the shapes of the standardized profiles rather than on a pointwise equality of numerical values. For each cluster  $C_g$ , the mean profile of explicit temporal perception is computed as

$$\overline{STP}_g(t) = \frac{1}{n_g} \sum_{i \in C_g} STP_i(t), \quad (28)$$

where  $n_g$  denotes the number of individuals belonging to cluster  $g$ . These mean STP profiles are then compared with the functional centroids of the centered trajectories  $\tau_i^c(t)$ , examining

their relative evolution across the observed temporal horizons. Since, in this study,  $\tau_i(t)$  are continuous-time functions while the STP measure is observed at discrete time points through the questionnaire, the comparison of their shapes requires a preliminary alignment step. To this end, the functional centroids of the centered curves  $\tau_i^c(t)$  are linearly interpolated at the temporal points corresponding to the STP observations. This makes it possible to perform the comparison using the same temporal references. The shape correlation between the standardized profile of  $\tau_i^c(t)$  and the standardized mean STP profile therefore provides a measure of the degree of correspondence between the implicit and explicit measures of subjective time within each cluster. The second level of the comparison concerns scalar relationships among the main quantitative indicators used in the study. In this regard, a Pearson correlation matrix is considered involving the individual discount rate  $k_i$ , the FPCA scores of the centered trajectories  $\tau_i^c(t)$ , the mean explicit temporal distance (mean STP), and additional psychometric indicators collected via questionnaire. This analysis allows for a description of the overall associative structure among implicit measures, explicit measures, and auxiliary variables related to subjective time perception. The comparison between implicit and explicit measures thus represents a complementary analysis with respect to the functional reconstruction, FPCA, and clustering. It allows for assessing whether the patterns of temporal deformation derived from intertemporal choices are also reflected in the reported representation of temporal distance. The aim is not to replace one measure with the other, but to understand whether they provide convergent, partially overlapping, or complementary information about subjective time perception.

## 5.7 Robustness Strategy

To assess the stability with respect to the main methodological choices, a robustness and sensitivity analysis of the clustering structure derived from the reconstructed subjective time trajectories was conducted. The stability of the solution was evaluated with respect to the number of functional principal components used for clustering, the specification of the clustering algorithm, the use of alternative functional distances and semi-metrics, the number of basis functions employed in the monotone smoothing procedures, and the treatment of functional outliers.

In the robustness analyses, the reference is given by the solution obtained in the main analysis based on the standardized FPCA scores computed on the centered functions  $\tau_i^c(t)$ , and it is taken as a benchmark for the subsequent analyses. The sensitivity with respect to the number of functional principal components was explored by progressively varying the number of FPCs used to construct the clustering space. The robustness with respect to the clustering procedure was assessed by considering different algorithmic configurations, including variations in the initializations of  $k$ -means, the use of the PAM method, and hierarchical clustering with Ward.D2 linkage. The sensitivity with respect to the choice of the distance measure was evaluated by comparing global distances on the centered functions and on the FPCA scores with semi-metrics based on the first and second derivatives of the trajectories. Finally, the stability with respect to the smoothing procedure was analyzed by

varying the number of basis functions used for monotone smoothing of  $f_i(t)$  and  $\tau_i(t)$ , in order to assess their impact on the resulting FPCA representation and clustering structure. The role of functional outlier treatment was also considered by examining the effect of excluding trajectories characterized by anomalous curvature patterns.

## 6 Empirical Application and Results

### 6.1 Functional reconstruction of discount curves and subjective time trajectories

The empirical analysis begins from the monetary equivalence judgments collected through the questionnaire, which are subsequently transformed into individual discount curves. For each participant, the reported equivalent amounts are first mapped into points of the empirical discount function  $f_i(t)$  and then processed through monotone decreasing smoothing. The resulting curves are then used to reconstruct individual subjective time functions  $\tau_i(t)$ , after estimating the individual discount scale  $k_i$  and imposing monotonicity and origin constraints on the subjective time function. The final functional sample consists of  $N = 107$  participants. Figure 1 summarizes the main graphical evidence from the reconstruction procedure. The upper-left panel displays the discount curves  $f_i(t)$ . Individual curves are shown in light blue, while the thick black line represents the sample mean. The average curve exhibits a slow but persistent decline, consistent with positive time preference, meaning that future outcomes are valued less than present ones. Individual heterogeneity is substantial. Some curves remain relatively high, indicating low impatience, while others decline rapidly, reflecting high impatience. The upper-right panel reports the subjective time functions  $\tau_i(t)$ . All functions start from zero, enforcing the constraint  $\tau_i(0) = 0$ , and increase monotonically. The diversity of observed shapes constitutes the main motivation for the FDA approach, since a fixed parametric specification would impose a restrictive structure on such heterogeneity. The lower panels report the first derivative  $\tau_i'(t)$  and the second derivative  $\tau_i''(t)$ , respectively. The first derivative describes the local speed of subjective time and, on average, tends to be higher in the short run and lower over longer horizons, a pattern consistent with decreasing impatience. Some individuals exhibit intermediate peaks or local reversals, suggesting more complex preference structures. The second derivative has a slightly negative sample mean, consistent with a prevailing pattern of decreasing impatience, while the dispersion around the mean indicates heterogeneous local dynamics. Overall, discount curves reveal marked heterogeneity in the valuation of future rewards, but subjective time functions show that this heterogeneity is not limited to discount intensity. Instead, individuals also differ in the overall shape of the temporal transformation. The first derivative captures the local speed of subjective time, whereas the second derivative captures changes in this speed across horizons. In this sense, the derivative-based representation allows one not only to assess whether subjective time increases, but also how sensitivity to temporal distance varies across short, medium, and long horizons. This initial graphical representation strengthens the central motivation of the functional approach. The analysis is not aimed solely at measuring how strongly individuals discount the future, but rather at characteriz-

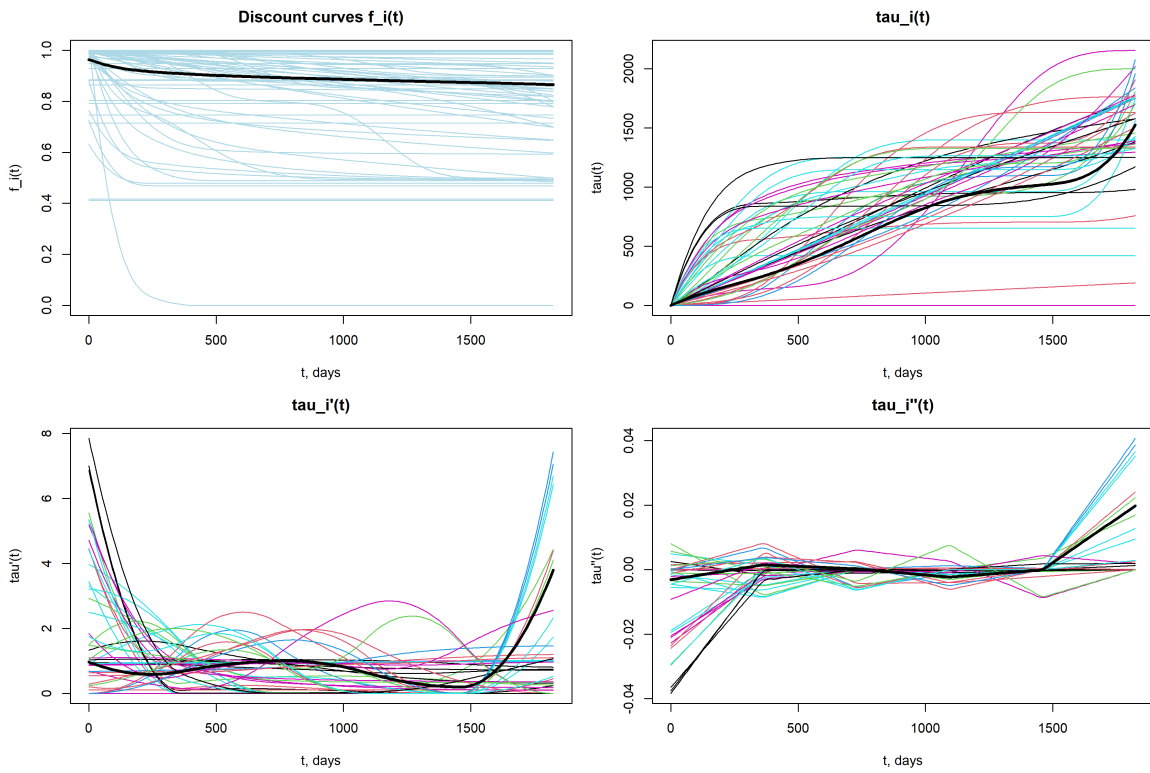


Figure 1: Functional reconstruction of discount curves and subjective time trajectories. The upper-left panel reports the smoothed discount curves  $f_i(t)$ ; the upper-right panel shows the recovered subjective time functions  $\tau_i(t)$ ; the lower panels display the first derivative  $\tau_i'(t)$  and the second derivative  $\tau_i''(t)$ , respectively. The final analytical sample consists of  $N = 107$  participants.

ing how chronological time is transformed into subjective time. The function  $\tau_i(t)$  therefore constitutes the main empirical object of the study, as it allows interindividual variability to be interpreted as a functional phenomenon rather than a simple scalar difference. The recovered trajectories should therefore be interpreted as normalized implicit subjective time functions, conditional on the individual discounting scale fixed by  $k_i$ , rather than as absolute psychophysical measures of perceived time.

## 6.2 Parametric benchmark analysis

To assess whether the functional reconstruction provides empirical information beyond standard parametric specifications, we compared the proposed FDA-based reconstruction with three benchmark models. The first benchmark is the classical exponential model defined on chronological time,  $f_i(t) = \exp(-k_i t)$ . The second is the Weber–Fechner subjective-time model,  $f_i(t) = \exp\{-k_i \alpha_i \log(1 + \beta_i t)\}$ , which implies a hyperbolic discounting form in objective time. The third is the Stevens power-law model,  $f_i(t) = \exp(-k_i \alpha_i t^{\beta_i})$ , which allows for concave or convex transformations of subjective time depending on the value of  $\beta_i$ .

The purpose of this comparison is not to reject parametric models, but to assess whether a fixed functional form is sufficient to represent the observed heterogeneity in individual discount trajectories. Model performance was evaluated at the individual level by comparing estimated values with the observed empirical discount factors at the questionnaire horizons. For each participant and for each model, the root mean squared error and the mean absolute error were computed. The FDA-based reconstruction was evaluated on the same temporal grid using the smoothed monotone discount trajectory. Consequently, RMSE and MAE should be interpreted as measures of in-sample reconstruction accuracy at the observed questionnaire horizons, rather than as measures of out-of-sample predictive performance.

This benchmark analysis provides a direct empirical check of the main methodological motivation of the paper. If parametric models perform similarly to the functional reconstruction for most individuals, the advantage of FDA mainly concerns interpretation, derivative analysis, FPCA, and clustering. Conversely, if the FDA reconstruction improves the representation of individual trajectories, especially for subjects exhibiting local curvature changes or non-standard deformation profiles, this supports the idea that subjective time heterogeneity is not fully reducible to a small number of parametric families.

The nonlinear parametric models were estimated at the individual level through constrained nonlinear least squares. Initial values, parameter bounds, and convergence diagnostics were monitored, and all models converged for the 107 participants included in the analytical sample. The comparison results are reported in Table 2. The exponential model defined on chronological time shows the largest errors, with a median RMSE equal to 0.02839 and a median MAE equal to 0.01653, and does not provide the best individual fit for any subject. Models based on subjective time transformations instead show substantially lower errors. The Weber–Fechner model presents a median RMSE equal to 0.00478 and a median MAE equal to 0.00387, resulting in the best individual fit for 68.2% of participants. The Stevens model presents a median RMSE equal to 0.00426 and a median MAE equal

to 0.00334, resulting in the best individual fit for 13.1% of participants. The FDA-based monotone reconstruction presents a median RMSE equal to 0.00463 and a median MAE equal to 0.00297, resulting in the best individual fit for 18.7% of participants.

These results indicate that parametric subjective time models constitute relatively simple benchmarks and, in many cases, are capable of accurately representing the observed individual trajectories. In particular, the Weber–Fechner model provides the best fit for the largest proportion of subjects. However, the FDA reconstruction maintains a distinct methodological role, since it allows the analysis of trajectory shapes, their derivatives, the FPCA structure, and functional clustering profiles.

Figure 2 provides a graphical diagnostic for six representative subjects, selected according to tertiles of the average parametric error, showing the observed points, the three parametric fits, and the FDA reconstruction over the same temporal horizons. This representation makes it possible to distinguish cases in which parametric benchmarks adequately describe the individual data from those in which local curvature, slope changes, or profiles not fully attributable to a single parametric family emerge.

Table 2: Parametric benchmark analysis. RMSE and MAE are computed at the thirteen questionnaire horizons. The percentage of best individual fit indicates the proportion of participants for whom each model attains the lowest RMSE.

Model	Median RMSE	Mean RMSE	Median MAE	Mean MAE	% best fit
Exponential objective time	0.02839	0.07317	0.01653	0.05526	0.0
Weber–Fechner logarithmic subjective time	0.00478	0.03022	0.00387	0.02442	68.2
Stevens power-law subjective time	0.00426	0.03120	0.00334	0.02529	13.1
FDA monotone reconstruction	0.00463	0.05028	0.00297	0.03916	18.7

### 6.3 FPCA of subjective time trajectories

Individual trajectories  $\tau_i(t)$  are then analyzed through Functional Principal Component Analysis applied to centered functions  $\tau_i^c(t) = \tau_i(t) - \bar{\tau}(t)$ , with the aim of identifying the main sources of variation around the sample mean trajectory and summarizing interindividual differences in subjective time deformation through a reduced number of functional dimensions. Figure 3 reports the first functional principal components and their explained variance. The FPCA decomposition shows that variability is strongly concentrated in the first two functional components. The first component explains 81.77% of total variance, whereas the second explains 15.66%. Together, the first two components account for 97.44% of total variability. Subsequent components explain only a residual share of variance. This indicates that heterogeneity in subjective time trajectories is low-dimensional and can be primarily described through a dominant functional mode of variation and a second component capturing more specific deviations along the temporal domain.

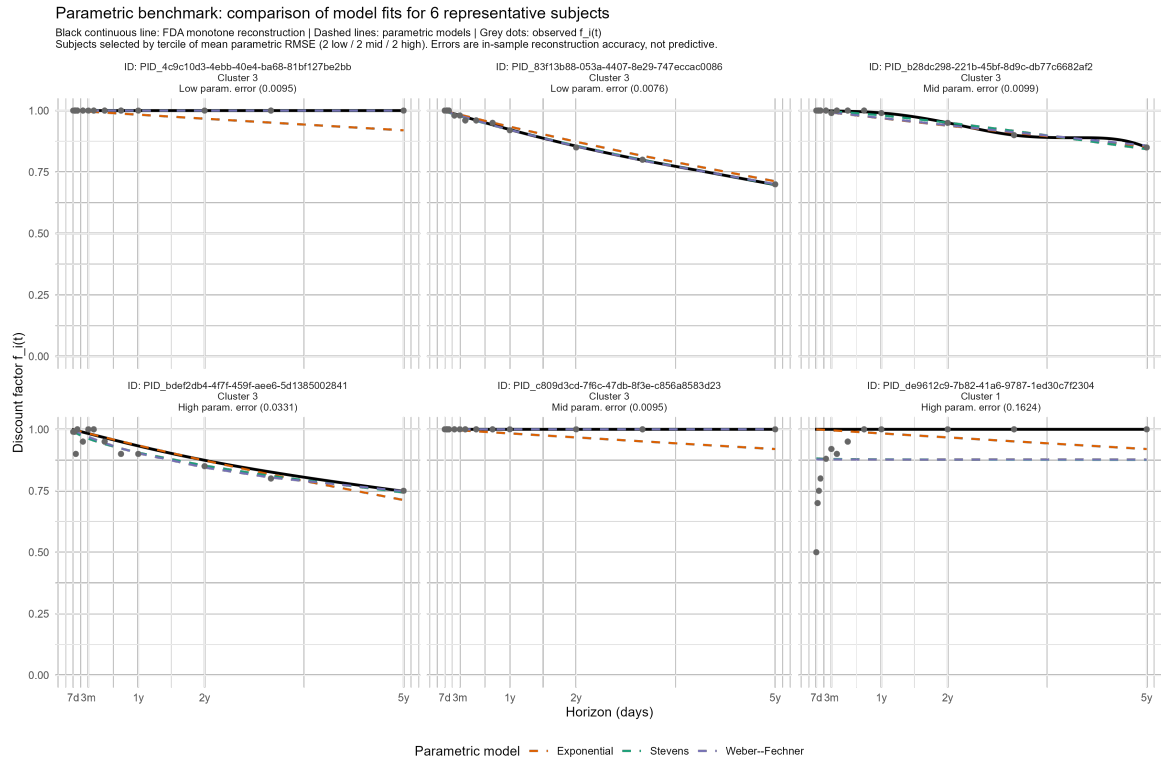


Figure 2: Diagnostic comparison between observed discount factors, parametric benchmark fits, and FDA monotone reconstruction for six representative subjects. Subjects are selected according to tertiles of the average parametric RMSE.

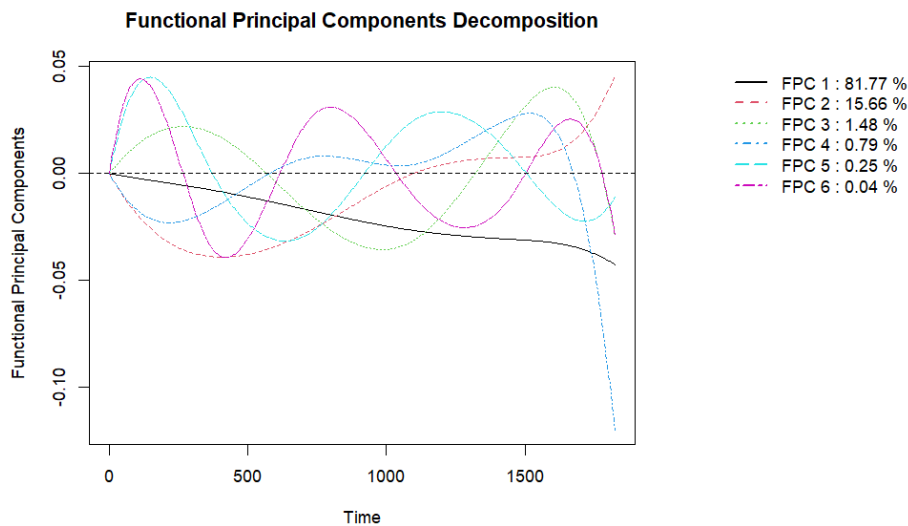


Figure 3: Functional Principal Component Analysis of centered subjective time trajectories. The figure reports the first functional principal components obtained from the centered functions  $\tau_i^c(t)$ , together with the percentage of variability explained by each component.

The first component can be interpreted as a global mode of deformation of subjective time relative to the sample mean. Given the sign convention returned by the FPCA algorithm, positive FPC1 scores correspond to trajectories lying below the sample mean, whereas negative scores correspond to trajectories lying above it. This sign convention is not substantive, since the sign of functional principal components is arbitrary and only affects the orientation used to describe the scores. The second component introduces a clearer distinction between short and long horizons, adding information on where deviations from the mean trajectory emerge along the time domain. A particularly relevant result concerns the relationship between the first FPCA score and the individual discount rate  $k_i$ . The Pearson correlation between FPC1 and  $k_i$  is  $r = -0.064$ , indicating a negligible association. This suggests that the dominant functional mode of subjective time deformation does not coincide with the scalar intensity of discounting. Individuals with similar  $k_i$  values may exhibit different shapes of  $\tau_i(t)$ , and individuals with different discount intensities may share similar deformation profiles. This finding supports the use of FDA as a complementary framework to the sole estimation of discount rates, since it highlights a source of heterogeneity that would remain largely unobserved when relying only on  $k_i$ .

#### 6.4 Functional Clustering of Subjective Time Profiles

FPCA scores are subsequently used to identify recurring patterns in subjective time deformation. Clustering is performed on standardized FPCA scores so that grouping relies on the main functional directions of variation, avoiding excessive dominance of the first component in cluster construction. The number of clusters is selected using the average silhouette criterion. The maximum silhouette value is obtained for  $k = 3$ , with an average silhouette of 0.801, whereas the solution with  $k = 4$  yields a lower value of 0.748, supporting the choice of three clusters. The three-cluster solution is further assessed through a bootstrap stability analysis based on 500 resamples. The mean Jaccard index equals 0.963 for Cluster 1, 0.928 for Cluster 2, and 0.969 for Cluster 3, indicating that the clustering structure remains stable across bootstrap samples. Cluster 2 shows slightly lower stability than the other two clusters, but its mean Jaccard value remains above 0.90. Cluster sizes are heterogeneous, with 18 subjects in Cluster 1 (16.8% of respondents), 22 in Cluster 2 (20.6%), and 67 in Cluster 3 (62.6%). Since clustering is applied to centered trajectories, groups should not be interpreted as absolute levels of subjective time, but rather as typical configurations of deviation from the sample mean trajectory. For this reason, clusters should not be interpreted as distinct “laws” of subjective time or as definitive psychological categories of individuals, but rather as exploratory functional profiles observed in the present sample. Positive centroid values indicate regions where the cluster lies above the mean trajectory, while negative values indicate regions below it. Figure 4 shows three distinct functional profiles. Cluster 1 exhibits a strongly negative and decreasing trend, starting near zero and progressively declining to values well below the sample mean. These individuals display  $\tau_i(t)$  systematically below the mean across the temporal domain, indicating a relative compression of subjective time, especially at longer horizons. Cluster 2 takes a bell-shaped profile, increasing rapidly up to

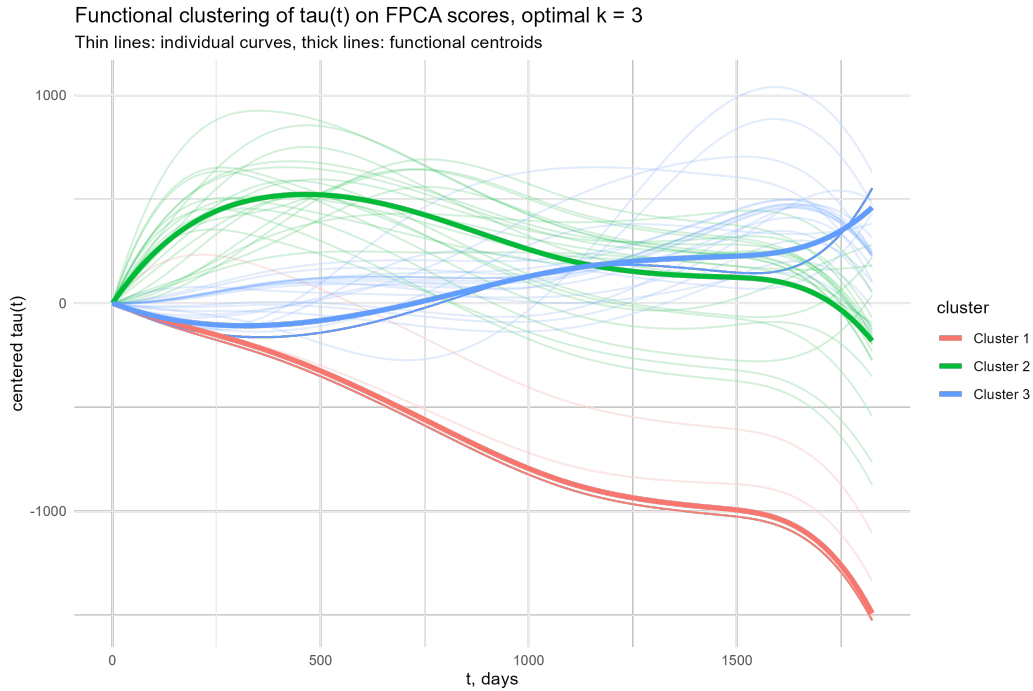


Figure 4: Functional clustering of centered subjective time trajectories. Thin lines represent individual centered trajectories  $\tau_i^c(t)$ , whereas thick lines represent the functional centroids of the clusters selected through the average silhouette criterion.

a peak around  $t = 300\text{--}400$  days and then declining progressively in the long run. These individuals show a relative expansion of time in the short-to-medium horizon, while perceiving the distant future as compressed relative to the mean. Cluster 3 shows an increasing and accelerated long-run trend, starting slightly below the mean and reaching values well above it at  $t = 1825$ , around  $+450$ . Short-run future time is perceived in line with the mean, whereas long-run time becomes progressively more expanded. These individuals perceive the distant future as farther than average. These results show that individual heterogeneity concerns not only discount intensity but also the shape of temporal deformation, that is, how subjective time deviates from the mean trajectory across different regions of the time domain. Clusters therefore capture functional profiles of subjective time rather than simple ordering by discounting intensity. External profiling of clusters is conducted using variables not included in the clustering procedure. These analyses are exploratory and descriptive, and the reported  $p$ -values, which are not adjusted for multiple comparisons, should be interpreted as descriptive indicators rather than confirmatory statistical tests. Mean age and TSS do not differ significantly across clusters, with ANOVA  $p$ -values of 0.803 and 0.957, respectively. Financial literacy shows a more pronounced descriptive pattern, with the highest average score observed in Cluster 2 (mean = 2.23), followed by Cluster 3 (mean = 1.79) and Cluster 1 (mean = 1.44). This result should not be taken as evidence that financial literacy explains or determines the identified subjective time profiles. Rather, it should be interpreted as a descriptive profiling pattern. The individual discount rate  $k_i$  also differs across clusters (ANOVA  $p = 0.011$ ), but this result must be interpreted jointly with the

near-zero correlation between FPC1 and  $k_i$  ( $r = -0.064$ ). The ANOVA indicates differences in average discount intensity across groups, while the correlation confirms that the dominant functional variation in  $\tau_i(t)$  does not correspond to a simple scalar effect of the discount rate. Overall, functional clustering shows that intertemporal differences emerge mainly in the structure of subjective time deformation, confirming that heterogeneity cannot be fully explained by  $k_i$  alone. Groups differ primarily in the shape and timing of subjective time deformation, indicating that intertemporal heterogeneity has a functional structure.

## 6.5 Supplementary parametric clustering comparison

As a supplementary benchmark, we additionally examined whether the functional clusters could be recovered from low-dimensional parametric summaries of subjective time. The purpose of this analysis is not to replace functional clustering, but to assess whether the groups identified from the complete trajectories  $\tau_i(t)$  are reducible to the parameters of standard subjective time models.

For each participant, the parameters estimated from the Weber–Fechner and Stevens specifications were used. Because the discounting scale and the subjective time scale enter the parametric specifications through the product  $k_i\alpha_i$ , the individual  $k_i$  estimated in the main FDA pipeline was used to derive the corresponding shape-scale parameter  $\alpha_i$  for the supplementary parametric clustering. Clustering was then conducted on standardized parametric vectors, considering both the complete set of parameters, including the discounting scale, and the shape parameters only. This distinction is relevant because it makes it possible to verify whether any agreement with the functional partition also depends on discounting intensity or mainly on the shape of the subjective time transformation. The number of clusters was fixed at three in order to allow a direct comparison with the functional partition obtained from the standardized FPCA scores. Agreement between the parametric partitions and the functional one was evaluated through the Adjusted Rand Index.

This comparison provides a diagnostic assessment of the relationship between parametric and functional representations. A high agreement would indicate that the functional groups are largely recoverable from parsimonious parametric summaries. Conversely, a moderate or low agreement would suggest that functional clustering captures additional shape information distributed along the temporal domain, including local curvature variations and deviations from the constraints imposed by logarithmic or power-law transformations. Therefore, the parametric clustering analysis should be interpreted as a supplementary robustness and interpretability check, rather than as an alternative classification strategy.

The results are reported in Table 3. The parametric spaces based on the Weber–Fechner model show very low agreement with the functional partition, both when considering  $k_i$ ,  $\alpha_i$ , and  $\beta_i$ , with an ARI equal to 0.006, and when considering only the shape parameters  $\alpha_i$  and  $\beta_i$ , with an ARI equal to  $-0.052$ . The parametric space based on the Stevens model instead shows a greater ability to partially recover the functional structure. In particular, k-means clustering on the parameters  $k_i$ ,  $\alpha_i$ , and  $\beta_i$  reaches an ARI equal to 0.522, whereas the use of the shape parameters only produces an ARI equal to 0.332. The supplementary control

based on PAM applied to the complete Stevens parametric space yields an ARI equal to 0.394.

These results indicate that the functional partition is not fully recoverable through low-dimensional parametric summaries. The Stevens model allows a partial reconstruction of the group structure, especially when the discounting scale is also included, but the agreement remains moderate. Consequently, functional clustering appears to capture additional information on the shape of subjective trajectories, distributed along the temporal domain and not fully reducible to the parameters of logarithmic or power-law transformations. This supports the use of functional clustering as the main exploratory tool for identifying recurring profiles of subjective time distortion.

**Table 3:** Supplementary parametric clustering comparison. The number of clusters is fixed at three to allow direct comparison with the functional clustering solution. Agreement is measured by the Adjusted Rand Index.

Parametric space	Algorithm	$k$	ARI	Interpretation
Weber–Fechner $(k_i, \alpha_i, \beta_i)$	k-means	3	0.006	Low agreement
Weber–Fechner $(\alpha_i, \beta_i)$ only	k-means	3	-0.052	Low agreement
Stevens $(k_i, \alpha_i, \beta_i)$	k-means	3	0.522	Moderate agreement
Stevens $(\alpha_i, \beta_i)$ only	k-means	3	0.332	Low agreement
Best parametric space, Stevens full	PAM	3	0.394	Low agreement

## 6.6 Comparison between Implicit and Explicit Subjective Time

A further analysis compares implicit subjective time trajectories  $\tau_i(t)$  with the explicit measure derived from the STP task, already introduced in previous sections. The analysis focuses on shapes rather than levels due to scale differences between the two measures and relates functional centroids of centered trajectories  $\tau_i^c(t)$  with standardized mean STP profiles at cluster level. Figure 5 shows that functional centroids of  $\tau(t)$  display strong shape heterogeneity, whereas STP profiles are more regular and less differentiated across clusters. Shape correlations between standardized  $\tau_i^c(t)$  centroids and standardized STP means are  $r_{C1} = -0.842$ ,  $r_{C2} = 0.085$ , and  $r_{C3} = 0.657$ , indicating a strong negative relation in Cluster 1, an almost null relation in Cluster 2, and a moderate positive relation in Cluster 3. These results indicate that convergence between implicit and explicit subjective time is only partial and cluster-specific. The comparison suggests a partial and heterogeneous relationship between implicit and explicit subjective time. However, these findings should be interpreted as an exploratory comparison between two related but distinct measures of subjective time, rather than as a direct validation of one measure through the other. Implicit trajectories derived from intertemporal choices capture a richer functional structure, while STP profiles provide a more direct but less differentiated representation of perceived temporal distance. This does not imply independence between the two measures, but rather that they describe different layers of subjective time perception. The correlation matrix of scalar variables provides a complementary perspective. The correlation between FPC1

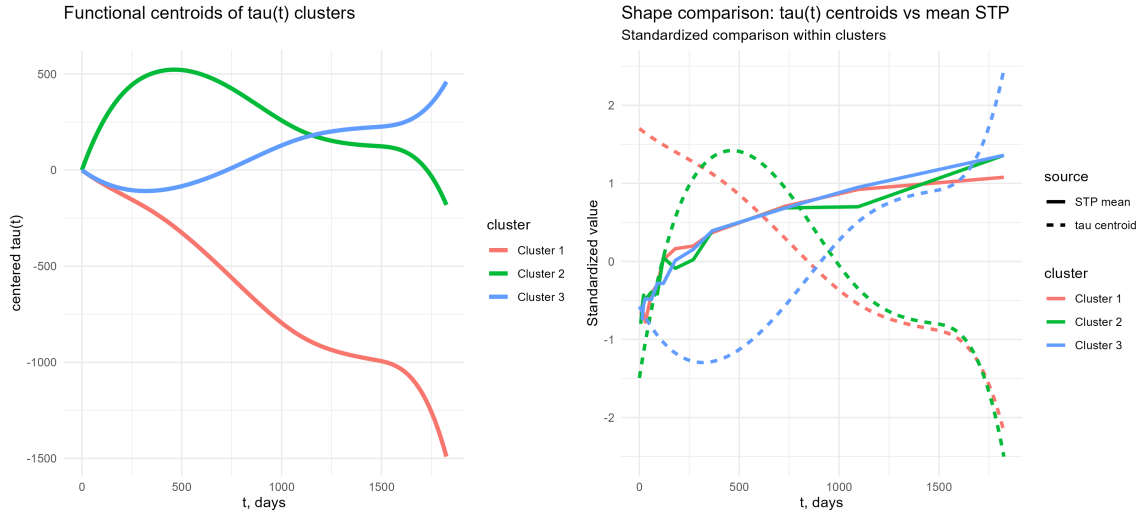


Figure 5: Comparison between implicit subjective time profiles and explicit STP profiles. The left panel reports the functional centroids of the  $\tau(t)$  clusters. The right panel compares the standardized shape of the  $\tau(t)$  centroids with the corresponding mean STP profiles within the same clusters.

and mean STP is  $r = -0.253$ , indicating a weak-to-moderate association. The correlation between TSS and mean STP is  $r = 0.010$ , essentially null, whereas the correlation between  $k_i$  and mean STP is  $r = 0.202$ , positive but modest. Overall, these results suggest that there is no single dimension that summarizes all measures of subjective time. Subjective time perception is therefore multidimensional, with implicit functional dynamics capturing more detailed structure than explicit reports.

## 6.7 Robustness and Sensitivity Analysis of the Clustering Solution

The results of the robustness analysis confirm that the main clustering structure does not depend on specific technical choices of the analytical procedure. The analysis yields three clusters based on standardized FPCA scores computed on the centered functions  $\tau_i^c(t)$ , which are used as a standard of reference for the alternatives considered in the sensitivity checks. Clustering is performed on standardized FPCA scores. This choice gives comparable weight to the retained functional components and prevents the first component from dominating the partition solely because of its larger variance. Geometrically, the procedure operates in a rescaled principal-component space rather than in the original variance-weighted  $L^2$  geometry. The robustness checks based on the  $L^2$  distance between centered trajectories yield highly concordant partitions, supporting the stability of the reference solution.

The first check concerns the number of functional principal components used to construct the clustering space. The main solution is based on the first two components, which jointly explain 97.44% of the variability of the centered trajectories. Increasing the number of components included in the analysis, the obtained partitions remain strongly aligned with the initial solution. In particular, the Adjusted Rand Index equals 1 when using three and four FPCs, while it remains high also when using five and six FPCs, with values equal to

0.838 and 0.811, respectively. In parallel, the average silhouette decreases as the number of included components increases, moving from 0.801 in the reference solution to 0.464 when six FPCs are used. This result suggests that the first functional components are already sufficient to capture the dominant cluster structure, while higher-order components mainly reduce group separation without substantially modifying the obtained partition.

The presence of a three-cluster structure is supported by both the selection of the optimal number of groups and the representation of the classification in the FPCA space. Figure 6 reports the average silhouette index as a function of the number of clusters  $k$ , used to support the choice of  $k = 3$  in the main analysis. The silhouette criterion identifies  $k = 3$  as the optimal solution, with an average value of 0.801, indicating a good separation between groups compared to the alternatives considered. The observed value for  $k = 4$  is lower (0.748), providing additional support for the three-cluster structure adopted in the main analysis.

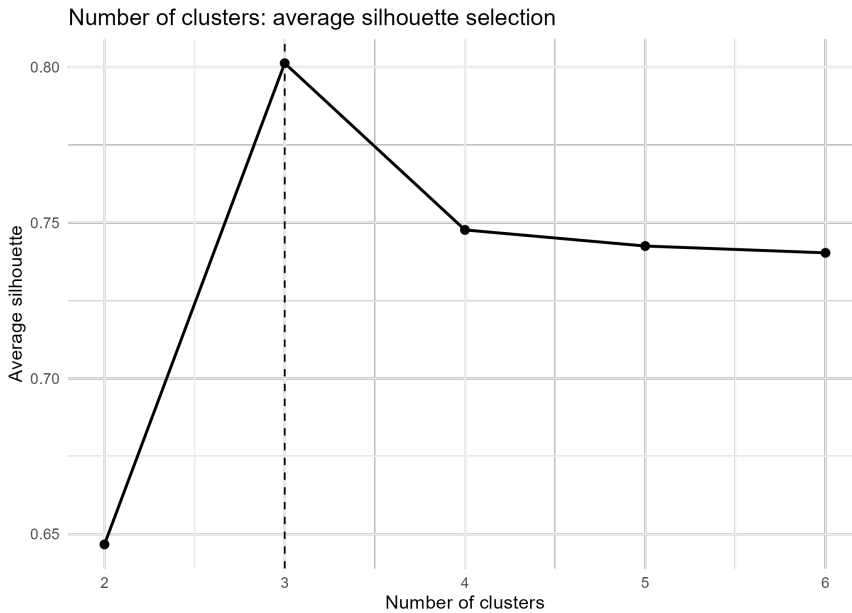


Figure 6: Average silhouette index as a function of the number of clusters  $k$  on standardized FPCA scores. The maximum is attained at  $k = 3$ , supporting the three-cluster solution adopted in the main analysis.

The distribution of subjects in the space of the first FPCA scores further shows that the three groups occupy distinct regions of the reduced space, indicating that the observed structure does not arise from isolated differences at specific time horizons, but from a functional configuration summarized by the principal components. Figure 7 provides a direct representation of the clustering structure in the space of the first two FPCA scores, allowing visualization of the arrangement of the three groups in the reduced-dimensional representation used for clustering. The separation observed in the FPCA score space further supports the interpretation that the clusters capture recurring modes of functional deviation from the sample mean trajectory.

The stability of the solution is assessed through a bootstrap procedure based on 500

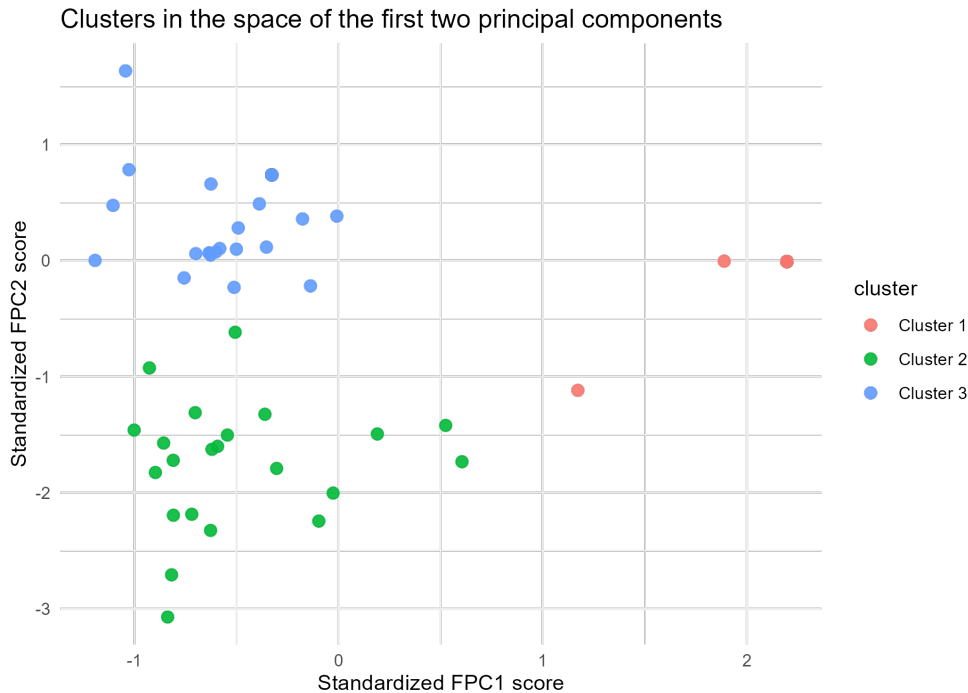


Figure 7: Scatterplot of the first two FPCA scores, with subjects colored according to the three-cluster solution. The plot provides a visualization of the clustering structure in the reduced-dimensional FPCA space.

resamples. The mean values of the Jaccard index are high for all three clusters, with values equal to 0.963 for Cluster 1, 0.928 for Cluster 2, and 0.969 for Cluster 3. These results indicate that the groups tend to maintain a high level of consistency across resampled datasets. Figure 8 provides a graphical summary of the bootstrap stability of the three-cluster solution, reporting the mean Jaccard similarity for each cluster.

To assess whether the obtained classification depends on the specific clustering procedure, a sensitivity analysis is conducted based on different algorithmic configurations. The three-cluster structure identified in the main solution remains unchanged when varying the number of random initializations of  $k$ -means and when using different versions of the algorithm. In all these cases, the Adjusted Rand Index with respect to the reference solution is equal to 1, indicating a complete match between the obtained partitions. The application of PAM on the distance between FPCA scores also reproduces the same partition, while hierarchical clustering with Ward.D2 linkage applied to the same distance yields a very similar solution, with an Adjusted Rand Index equal to 0.955. Taken together, these results show that the cluster structure is not the product of a specific random initialization nor of a particular implementation of  $k$ -means, but reflects a stable configuration present in the data. The graphical results of these checks are reported in Appendix in Figures 16 and 17.

An additional check concerns the choice of the distance measure used to compare the subjective trajectories. When clustering is performed using the  $L^2$  distance on the centered functions  $\tau_i^c(t)$ , the results are highly similar to the reference solution in terms of cluster structure, with Adjusted Rand Index values equal to 0.968 for PAM and 0.955 for Ward.D2.

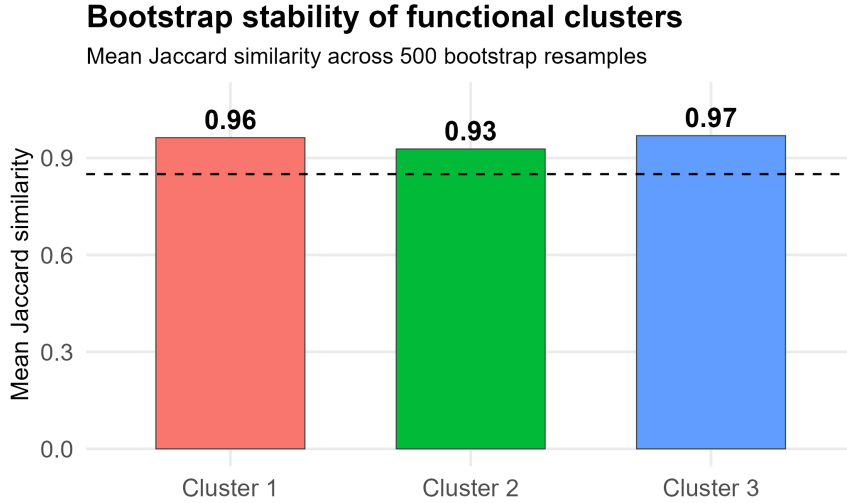


Figure 8: Graphical representation of the bootstrap stability of the three-cluster solution. The figure reports the mean Jaccard similarity for each functional cluster across bootstrap resamples. Higher values indicate greater cluster stability.

Similar results are also obtained using the Euclidean distance on standardized FPCA scores, with values equal to 1 for PAM and 0.955 for Ward.D2. A different situation emerges when clustering is based on semi-metrics defined on the derivatives of the functions. In particular, the Adjusted Rand Index ranges between 0.436 and 0.499 for the first derivative and equals 0.335 for the second derivative. This result suggests that derivative-based semi-metrics highlight different aspects of the functional trajectories, more closely related to local variation speed and curvature, producing partitions that do not necessarily coincide with those obtained when considering the global shape of  $\tau_i^c(t)$ . These results do not contradict the reference solution and clarify that the main clustering structure is mainly associated with the overall shape of the subjective time deformation, while derivatives describe a more local and dynamic level of information. In Appendix, Figure 18 shows the complementary role of derivative information with respect to global functional distances.

Finally, the stability of the results is considered with respect to the number of basis functions used in the monotone smoothing step. The procedure employs 10 basis functions for the decreasing monotone smoothing of  $f_i(t)$  and 8 basis functions for the increasing monotone smoothing of  $\tau_i(t)$ . Alternative specifications are evaluated by varying the number of basis functions for  $f_i(t)$  between 8, 10, and 12, and for  $\tau_i(t)$  between 6, 8, and 10. Across the nine considered combinations, the Adjusted Rand Index with respect to the reference solution is always equal to either 0.968 or 1. Moreover, the proportion of variance explained by the first FPC remains between 0.809 and 0.830, whereas the cumulative variance explained by the first two FPCs ranges between 0.974 and 0.992. These results show that the main structure derived from FPCA and the clustering solution are not substantially affected by moderate changes in the smoothing basis specification.

Overall, the set of checks confirms the robustness of the main empirical findings. Of the 29 performed checks, 25 yield an Adjusted Rand Index of at least 0.80 with respect to

the reference solution, with a median equal to 1. The lowest values are observed only in analyses based on derivative semi-metrics, which are designed to capture more local and dynamic features of the curves. Taken together, these results indicate that the clustering structure is not sensitive to the main choices of the FDA pipeline, including the number of FPCs, the clustering specification, the use of global functional distances, and the smoothing basis configuration. At the same time, the observed sensitivity of derivative-based semi-metrics suggests that local dynamics of subjective time provide complementary information, to be interpreted as an additional descriptive layer with respect to the reference solution.

## 7 Discussion

This study analyzed the deformation of subjective time by integrating discounting theory with Functional Data Analysis, interpreting subjective time as an individual functional trajectory in intertemporal choices. The central contribution of the study consists in introducing a functional representation of the subjective transformation of time in place of a scalar description of intertemporal preferences. Starting from equivalence judgments between an immediate reward and a fixed future amount, empirical discount curves are reconstructed, subsequently regularized through monotonicity constraints and transformed into individual functions of subjective time  $\tau_i(t)$ . Objective time is not considered merely as an external variable in the decision-making process, but as a component that can take different subjective configurations along the entire temporal horizon. Functional Data Analysis makes it possible to study the subjective transformation of time without imposing a specific parametric form in advance, allowing the overall shape, local variations, dimensional structure, and possible recurring profiles to be analyzed [14, 18].

An interpretative aspect concerns the heterogeneity observed across individuals. The results suggest that differences in intertemporal choices cannot be adequately described solely through the intensity of discounting or by a single individual parameter  $k_i$ . The function  $\tau_i(t)$  shows that individuals may perceive the future in different ways, even when they exhibit similar levels of discounting. Indeed, two subjects may present similar values of the parameter  $k_i$  but differ in the shape of the subjective trajectory, especially in those regions of the time domain where the future is perceived as more compressed, expanded, or more relevant from a decision-making perspective. For this reason,  $k_i$  can be interpreted as an operational scaling parameter, whereas  $\tau_i(t)$  is treated as the main functional object of interest, without assuming a strict separation between the two components. In the model  $f_i(t) = \exp\{-k_i\tau_i(t)\}$ , discounting and time perception jointly interact through the product  $k_i\tau_i(t)$ . The aim of the analysis is therefore not to separate these two effects, but to provide an interpretable representation of individual temporal deformation.

The analysis of derivatives allows this interpretation to be further refined. The first derivative  $\tau_i'(t)$  captures the local speed of subjective time, whereas the second derivative  $\tau_i''(t)$  describes the acceleration of the function and thus the change in this speed along the temporal horizon. In this sense,  $\tau_i(t)$  is not interpreted only as an increasing curve, but

as a dynamic function in which changes in intensity, slowdowns, and accelerations in the perception of temporal distance can be observed. When the second derivative is negative, it suggests that temporal sensitivity decreases progressively over time, in line with decreasing impatience, whereas positive values indicate a local increase in sensitivity to temporal distance [2, 18]. This result is relevant because it links the functional representation of subjective time to the literature on intertemporal anomalies, without reducing these phenomena to simple deviations from a constant discount rate.

The Functional Principal Component Analysis (FPCA) results provide an additional level of interpretation. Despite the evident variability across individual trajectories, the centered functions of subjective time exhibit an overall low-dimensional structure. The first functional component captures the main mode of deviation of subjective time deformation with respect to the sample mean, whereas the second component introduces additional information on differences between short and long time horizons. Individual differences are not spread across many independent directions but can instead be summarized by a limited number of main functional directions. The near-zero correlation between the first FPCA score and the parameter  $k_i$  suggests that the dominant structure of  $\tau_i(t)$  does not coincide with the scalar intensity of discounting. From a methodological perspective, this result shows that FPCA is an appropriate dimensionality reduction tool, as it preserves the main information on curve shape and allows functional representations to be used in subsequent analyses [10, 14].

The parametric benchmark analysis clarifies the role of the functional approach. The results do not suggest that classical subjective-time models are inadequate; on the contrary, logarithmic and power-law specifications provide accurate and interpretable approximations for many individual trajectories. However, their parameters do not fully recover the functional clustering structure obtained from the complete trajectories. This indicates that the FDA framework adds information not merely in terms of reconstruction accuracy, but in terms of shape analysis, derivative-based interpretation, dimensional decomposition, and the detection of recurrent temporal-deformation profiles along the whole time domain.

Functional clustering adds another layer of interpretation to the data. Clusters should not be understood neither as representations of different laws of subjective time, nor as evidence of separate models for distinct groups of individuals. They instead provide a reconstruction of individual trajectories within a single common functional space. The mean function describes the average subjective transformation of time, whereas clusters highlight recurring forms of deviation from this mean. This interpretation allows individual heterogeneity to be described without replacing the common structure of the phenomenon with a rigid classification. The three identified profiles can therefore be interpreted as recurring modes of subjective time deformation, characterized by a systematic compression of the future, a progressive expansion of distant horizons, and a bell-shaped profile with greater relevance of short and intermediate horizons. In this sense, differences across individuals concern not only how much the future is discounted, but also when, along the time domain, the future becomes subjectively closer, more distant, or more relevant. The external profiling of clusters suggests further interpretative insights, although it remains exploratory

in nature. Differences across clusters with respect to age and the Temporal Sense Scale are not significant, whereas financial literacy shows a more pronounced descriptive pattern, with the highest average value observed in the cluster characterized by a bell-shaped profile and greater relevance of short- and intermediate-term horizons. This result suggests that financial literacy may be associated not simply with lower impatience in a scalar sense, but with a different functional organization of temporal perception. This interpretation should be treated with caution, given the exploratory nature of the analysis and the limited size of some groups. Nevertheless, the result points to a possible research direction in which cognitive skills, individual characteristics, and psychological variables are studied not only in relation to the average level of impatience, but also in relation to the shape of the subjective time function.

The comparison between implicit and explicit subjective time represents another contribution to the study. The function  $\tau_i(t)$  is derived from intertemporal choices and therefore reflects an implicit measure of the temporal structure embedded in decision-making behavior. The STP measure, instead, is derived from an explicit task assessing perceived temporal distance. The results show only partial convergence between the two measures, limited to specific clusters. The profiles of  $\tau_i(t)$  exhibit greater heterogeneity in shape, whereas STP profiles are more regular and less differentiated across groups. This result does not imply independence between the two measures, but rather suggests that they capture different levels of subjective time representation. The implicit measure appears to capture a richer structure that depends on the temporal horizon, whereas the explicit measure appears more direct but less discriminative. The weak convergence between TSS and mean STP further confirms that even explicit measures of temporal subjectivity do not necessarily reduce to a single dimension. Overall, the comparison suggests that subjective time should be considered a multidimensional construct in which choice behavior, stated temporal distance, and perceived time speed provide complementary information.

The robustness checks reinforce the interpretation of the main results. The clustering structure is stable with respect to variations in the number of functional principal components used, the specification of the clustering algorithm, the use of global functional distances, and moderate changes in the number of basis functions used in smoothing procedures. This indicates that the obtained profiles do not depend on a specific technical decision in the FDA pipeline. At the same time, derivative-based semimetrics produce partitions that are less aligned with the reference solution, suggesting that local speed and curvature of trajectories contain complementary information with respect to the global shape of  $\tau_i(t)$ . This result clarifies that the deformation of subjective time can be analyzed at different levels, a global one related to the overall shape, and a local one related to variation dynamics.

Some interpretative cautions are nevertheless necessary. Clustering should be considered exploratory in nature and interpreted as a descriptive tool useful for summarizing recurring functional configurations, without being understood as a definitive classification of individuals. The relationship between  $k_i$  and  $\tau_i(t)$  is defined through an operational normalization procedure, so the two components cannot be interpreted as fully independent in an absolute

sense. The partial correspondence between  $\tau_i(t)$  and STP may stem either from a genuine distinction between implicit and explicit subjective time, or from characteristics of the STP measure, such as scaling effects, response noise, or limited task sensitivity. It should also be noted that the analyzed sample is small, and some external profiling analyses should be regarded as descriptive. For this reason, larger samples and more structured validation designs are required to assess the stability of functional profiles and their relationships with psychological, behavioral, and socio-demographic variables.

Overall, the proposed approach shows how the integration of intertemporal choice theory and Functional Data Analysis offers a flexible perspective for reconstructing and studying subjective time as a functional object. By combining monotone smoothing, derivative analysis, FPCA, clustering, comparison with explicit STP measures, and robustness checks, the study provides a structured approach to analyzing variability in temporal perception across individuals. The main contribution does not lie solely in estimating individual discount curves, but in the possibility of analyzing the functional organization of perceived time and its role in intertemporal decision-making processes.

## 8 Conclusions and Future Developments

The results of the present study show that the functional modelling of subjective time makes it possible to analyze intertemporal choices beyond the sole intensity of discounting. The main contribution of the study does not concern only the reconstruction of individual discount curves, but also the possibility of interpreting the subjective transformation of time as an individual functional trajectory. Through the function  $\tau_i(t)$ , it is possible to observe how time is subjectively perceived across different temporal horizons, assuming configurations of compression, expansion, or greater local relevance. The results further show that intertemporal heterogeneity cannot be explained solely through the parameter  $k_i$ , since the structure of the trajectories, derivatives, FPCA, and clustering highlight differences not only in the level of discounting, but also in the form and dynamics of temporal deformation. This aspect represents the main methodological contribution of the study, as it makes it possible to analyze subjective time perception as a continuous and structured phenomenon, rather than as an isolated scalar measure. Moreover, the comparison between implicit subjective time and explicit measures of temporal perception suggests that subjective time cannot be reduced to a single observable dimension, since the functions  $\tau_i(t)$  and the STP measures show only partial convergence and appear to reflect complementary aspects of the subjective representation of time. These findings should be interpreted in light of the observational nature of the study, the final analytical sample of  $N = 107$  participants, and the use of a multilingual questionnaire. Therefore, they should not be read as causal evidence or as directly generalizable to broader populations without further replication. Future developments may deepen these findings in several directions. One possible extension concerns the application of the proposed approach to larger and more heterogeneous samples, in order to evaluate the stability of the reconstructed trajectories and the identified functional profiles.

Further developments may derive from the use of functional regression models or functional ANOVA approaches, which may be useful for systematically analyzing the relationship between the shape of the functions  $\tau_i(t)$  and individual covariates, such as financial literacy, health conditions, lifestyle habits, future orientation, and socio-demographic characteristics. The comparison between implicit and explicit measures of subjective time could also be further explored. In summary, the proposed approach combines intertemporal choice theory and Functional Data Analysis by focusing on the form of subjective time deformation. Considering subjective time as a functional trajectory makes it possible to describe dimensions of individual heterogeneity that would remain difficult to observe through models based exclusively on scalar parameters. In this sense, the proposed contribution offers new directions for the study of intertemporal inconsistency and for the analysis of subjective time perception in decision-making processes.

## Funding

The authors received no financial support for the research, authorship, or publication of this article.

## Competing Interests

The authors declare that they have no financial or non-financial competing interests related to the subject matter of this manuscript.

## References

- [1] Salvador Cruz Rambaud and Isabel González Fernández. A new approach to intertemporal choice: The delay function. *Symmetry*, 12(5):807, May 2020. ISSN 2073-8994. doi: 10.3390/sym12050807. URL <http://dx.doi.org/10.3390/sym12050807>.
- [2] Salvador Cruz Rambaud and Javier Sánchez García. A formal analysis of inconsistent decisions in intertemporal choice through subjective time perception. *Heliyon*, 9(11):e21077, November 2023. ISSN 2405-8440. doi: 10.1016/j.heliyon.2023.e21077. URL <http://dx.doi.org/10.1016/j.heliyon.2023.e21077>.
- [3] Salvador Cruz Rambaud, Piedad Ortiz Fernández, and Isabel María Parra Oller. A systematic review of the main anomalies in intertemporal choice. *Journal of Behavioral and Experimental Economics*, 104:101999, June 2023. ISSN 2214-8043. doi: 10.1016/j.socec.2023.101999. URL <http://dx.doi.org/10.1016/j.socec.2023.101999>.
- [4] Serge Galam. Measuring the subjective passage of time: A sociophysics modeling. *Entropy*, 26(6):528, June 2024. ISSN 1099-4300. doi: 10.3390/e26060528. URL <http://dx.doi.org/10.3390/e26060528>.
- [5] B. Kyu Kim and Gal Zauberman. Perception of anticipatory time in temporal discounting. *Journal of Neuroscience, Psychology, and Economics*, 2(2):91–101, November

2009. ISSN 1937-321X. doi: 10.1037/a0017686. URL <http://dx.doi.org/10.1037/a0017686>.
- [6] B. Kyu Kim and Gal Zauberman. Psychological time and intertemporal preference. *Current Opinion in Psychology*, 26:90–93, April 2019. ISSN 2352-250X. doi: 10.1016/j.copsyc.2018.06.005. URL <http://dx.doi.org/10.1016/j.copsyc.2018.06.005>.
- [7] G. Loewenstein and D. Prelec. Anomalies in intertemporal choice: Evidence and an interpretation. *The Quarterly Journal of Economics*, 107(2):573–597, May 1992. ISSN 1531-4650. doi: 10.2307/2118482. URL <http://dx.doi.org/10.2307/2118482>.
- [8] George Loewenstein and Richard H. Thaler. Anomalies: Intertemporal choice. *Journal of Economic Perspectives*, 3(4):181–193, November 1989. ISSN 0895-3309. doi: 10.1257/jep.3.4.181. URL <http://dx.doi.org/10.1257/jep.3.4.181>.
- [9] Roberta Martino, Annamaria Porreca, Viviana Ventre, and Fabrizio Maturo. Exploring intertemporal decision-making dynamics through functional data analysis: investigating variations in different discount function’s dimensions. *Quality & Quantity*, 59(3):2171–2196, April 2024. ISSN 1573-7845. doi: 10.1007/s11135-024-01869-y. URL <http://dx.doi.org/10.1007/s11135-024-01869-y>.
- [10] Fabrizio Maturo and Rosanna Verde. Combining unsupervised and supervised learning techniques for enhancing the performance of functional data classifiers. *Computational Statistics*, 39(1):239–270, July 2022. ISSN 1613-9658. doi: 10.1007/s00180-022-01259-8. URL <http://dx.doi.org/10.1007/s00180-022-01259-8>.
- [11] Fabrizio Maturo, Annamaria Porreca, Viviana Ventre, Roberta Martino, and Salvador Cruz Rambaud. Functional clustering of discount functions for behavioural investor profiling. *Applied Stochastic Models in Business and Industry*, 42(3), May 2026. ISSN 1526-4025. doi: 10.1002/asmb.70101. URL <http://dx.doi.org/10.1002/asmb.70101>.
- [12] James J. McGrath and James F. O’Hanlon. Method for measuring the rate of subjective time. *Perceptual and Motor Skills*, 24(3):1235–1240, June 1967. ISSN 1558-688X. doi: 10.2466/pms.1967.24.3c.1235. URL <http://dx.doi.org/10.2466/pms.1967.24.3c.1235>. Suppl.
- [13] Drazen Prelec. Decreasing impatience: A criterion for non-stationary time preference and “hyperbolic” discounting. *The Scandinavian Journal of Economics*, 106(3):511–532, October 2004. ISSN 1467-9442. doi: 10.1111/j.0347-0520.2004.00375.x. URL <http://dx.doi.org/10.1111/j.0347-0520.2004.00375.x>.
- [14] J. O. Ramsay and B. W. Silverman. *Functional Data Analysis*. Springer New York, 2005. ISBN 9780387227511. doi: 10.1007/b98888. URL <http://dx.doi.org/10.1007/b98888>.

- [15] Paul A. Samuelson. A note on measurement of utility. *The Review of Economic Studies*, 4(2):155, February 1937. ISSN 0034-6527. doi: 10.2307/2967612. URL <http://dx.doi.org/10.2307/2967612>.
- [16] Taiki Takahashi, Hidemi Oono, and Mark H. B. Radford. Psychophysics of time perception and intertemporal choice models. *Physica A: Statistical Mechanics and its Applications*, 387(8-9):2066–2074, March 2008. ISSN 0378-4371. doi: 10.1016/j.physa.2007.11.047. URL <http://dx.doi.org/10.1016/j.physa.2007.11.047>.
- [17] Richard Thaler. Some empirical evidence on dynamic inconsistency. *Economics Letters*, 8(3):201–207, January 1981. ISSN 0165-1765. doi: 10.1016/0165-1765(81)90067-7. URL [http://dx.doi.org/10.1016/0165-1765\(81\)90067-7](http://dx.doi.org/10.1016/0165-1765(81)90067-7).
- [18] Viviana Ventre, Roberta Martino, Salvador Cruz Rambaud, Fabrizio Maturo, and Annamaria Porreca. An original approach to anomalies in intertemporal choices through functional data analysis: Theory and application for the study of hikikomori syndrome. *Socio-Economic Planning Sciences*, 92:101840, April 2024. ISSN 0038-0121. doi: 10.1016/j.seps.2024.101840. URL <http://dx.doi.org/10.1016/j.seps.2024.101840>.
- [19] Gal Zauberman, B. Kyu Kim, Selin A. Malkoc, and James R. Bettman. Discounting time and time discounting: Subjective time perception and intertemporal preferences. *Journal of Marketing Research*, 46(4):543–556, August 2009. ISSN 1547-7193. doi: 10.1509/jmkr.46.4.543. URL <http://dx.doi.org/10.1509/jmkr.46.4.543>.

# Appendix

## Supplementary Material

This appendix reports additional methodological details and supplementary graphical evidence related to the functional reconstruction of subjective time, its representation through FPCA, the clustering procedure, the comparison between implicit and explicit subjective time, and the robustness analyses. The aim is not to introduce new empirical results, but to provide greater transparency on the analytical workflow and to support the interpretation of the results presented in the main text.

Figure 9 reports the distribution of the discount factor  $f_i(t) = A_{0,i}(t)/100$  for each of the thirteen time horizons considered. Median values show a progressive reduction as delay increases, consistent with the presence of positive time preference in the sample. Individual heterogeneity is marked across all horizons, with dispersion tending to increase for longer delays.

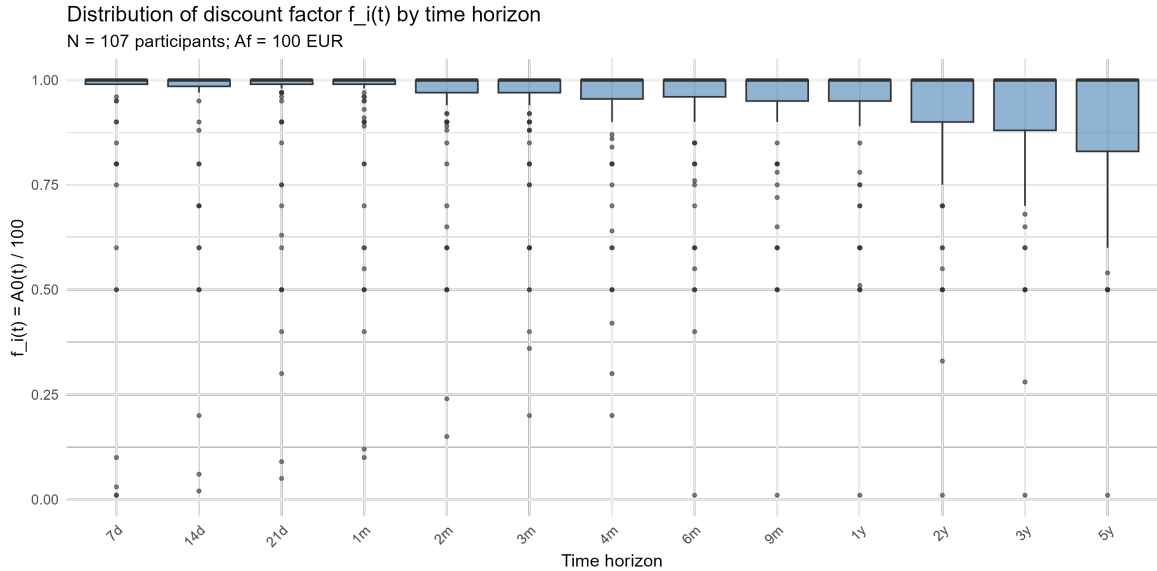


Figure 9: Distribution of the discount factor  $f_i(t)$  by time horizon. Boxplots report the median, quartiles, and extreme values for each of the thirteen questionnaire horizons.  $N = 107$ .

Figure 10 reports the distribution of STP responses for each time horizon, expressed in subjective months after normalization on the individual 7-day anchor. Median values increase with the objective horizon but in a markedly sublinear fashion. Dispersion increases substantially for longer horizons, reflecting greater individual variability in the perception of the distant future.

Figure 11 reports the distribution of the five core items of the Temporal Sense Scale used to compute the TSS index. Mean values range between 4 and 6 across all items, indicating a perceived time speed slightly above neutral in the sample.

Table 4 reports the missing rate by variable block in the analytical sample. The missing rate is zero for equivalence and STP variables, and between 1.9% and 2.8% for TSS items,

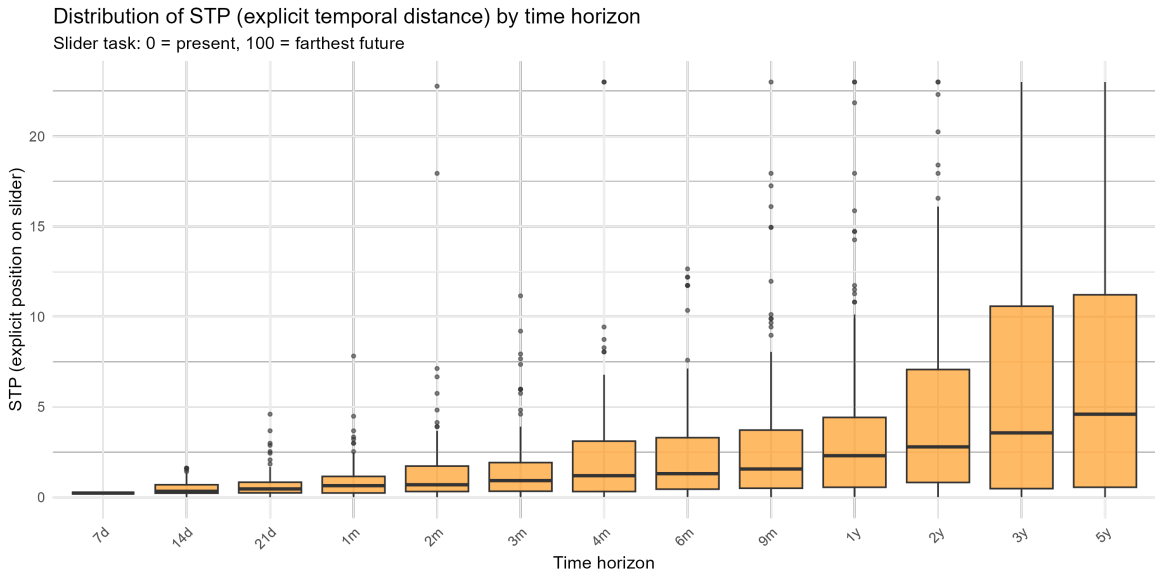


Figure 10: Distribution of STP responses by time horizon, expressed in subjective months normalized on the individual 7-day anchor.  $N = 107$ .

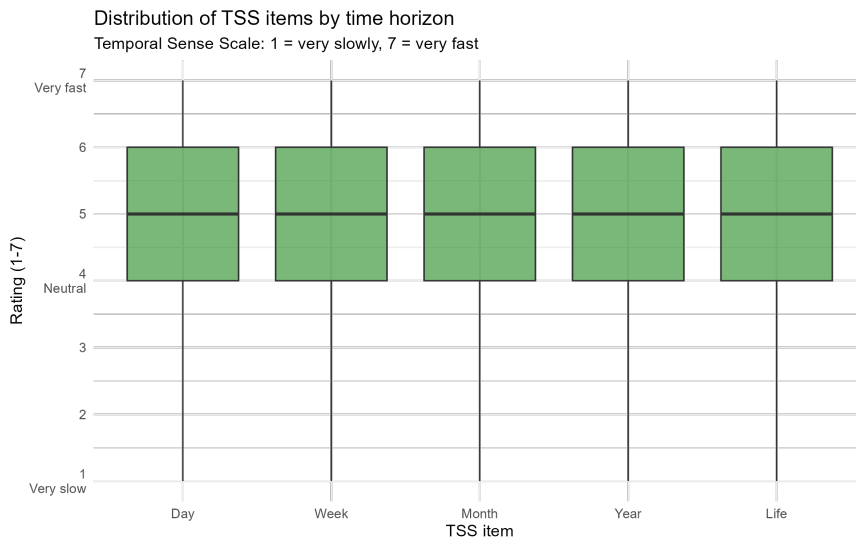


Figure 11: Distribution of core Temporal Sense Scale items by temporal window. The scale ranges from 1 (very slowly) to 7 (very fast).  $N = 107$ .

a negligible value that did not require imputation procedures.

Table 4: Missing rate by variable block in the analytical sample ( $N = 107$ ).

Block	Variables	N missing	% missing
Equivalence	eq_7d – eq_5y (13 items)	0	0.0
STP	stp_7d – stp_5y (13 items)	0	0.0
TSS	tss_day	3	2.8
	tss_week	3	2.8
	tss_month	2	1.9
	tss_year	2	1.9
	tss_life	3	2.8

Figure 12 reports the distribution of individual discount rates  $k_i$  in the analytical sample. The distribution is right-skewed, with the majority of participants concentrated at low values (mean = 0.000212, median = 0.000021), and a small number of subjects showing substantially higher discount rates. This pattern is consistent with the presence of marked individual heterogeneity in discounting intensity.

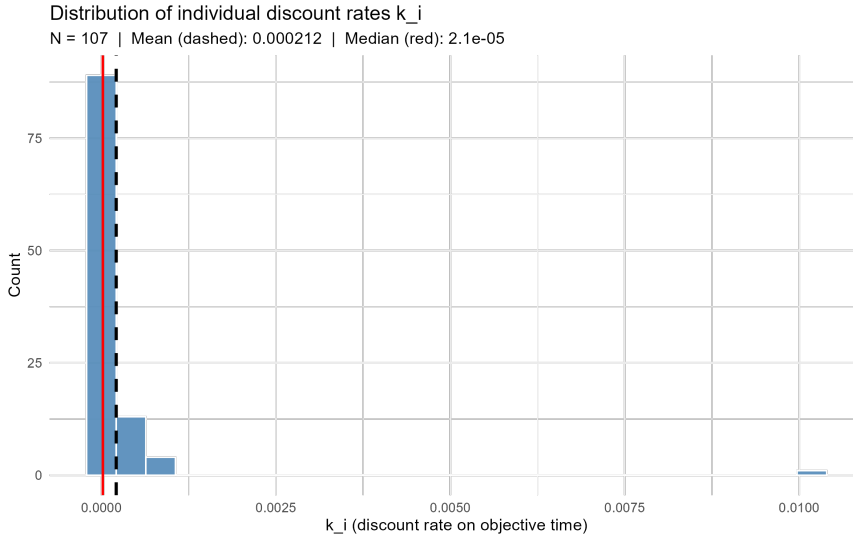


Figure 12: Distribution of individual discount rates  $k_i$  in the analytical sample. The dashed vertical line indicates the mean; the solid red line indicates the median.  $N = 107$ .

Table 5 reports the bootstrap stability results for the three-cluster solution, based on 500 resamples. For each cluster, the table reports the Mean Jaccard similarity between the original solution and the bootstrap solutions, the number of dissolution episodes, resamples with Jaccard ( $< 0.5$ ), and the number of recovery episodes, resamples with Jaccard ( $> 0.75$ ). All three clusters show mean Jaccard values above 0.90, confirming the stability of the solution. Cluster 2 shows a slightly higher number of dissolution episodes relative to the other clusters, although its mean Jaccard value remains high. Figure 13 reports the Pearson correlation matrix among the main scalar quantities used in the empirical analysis, including

Table 5: Bootstrap stability of the three-cluster solution. The table reports the mean Jaccard similarity for each functional cluster across 500 bootstrap resamples, together with dissolution and recovery counts. Higher mean Jaccard values indicate greater cluster stability.

Cluster	Mean Jaccard similarity	Dissolution count	Recovery count
Cluster 1	0.963	6	478
Cluster 2	0.928	45	454
Cluster 3	0.969	0	475

the individual discount rate  $k_i$ , the first two FPCA scores of the centered subjective time trajectories, the TSS core index, and the mean STP measure. The matrix provides a compact summary of the relationships between implicit functional measures, explicit time-perception measures, and the scalar discounting parameter. The weak correlations observed among most constructs support the interpretation that these quantities capture related but non-equivalent dimensions of subjective time and intertemporal choice.

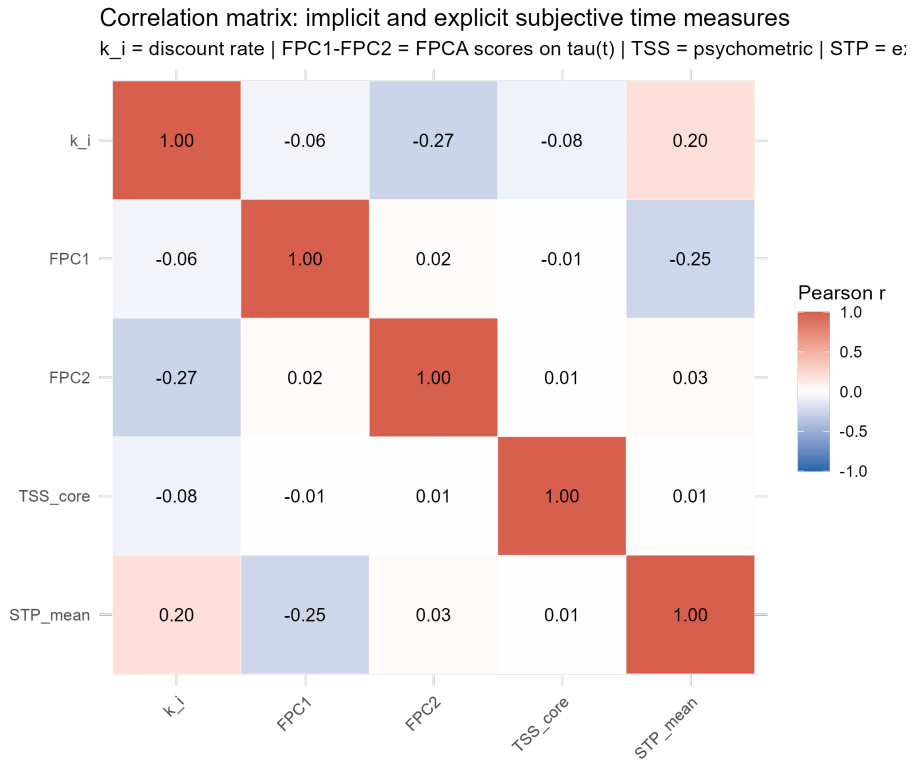


Figure 13: Pearson correlation matrix among  $k_i$ , FPCA scores, TSS core index, and mean STP. The heatmap summarizes the association structure between implicit subjective time measures, explicit time-perception measures, and the scalar discount rate.

Figure 14 focuses on the relationship between the first FPCA score and the mean STP measure. This comparison provides a supplementary graphical representation of the association between the dominant functional mode of implicit subjective time deformation and the explicit measure of perceived temporal distance. The observed pattern is consistent with the

interpretation developed in the main text, according to which implicit and explicit subjective time are only partially aligned.

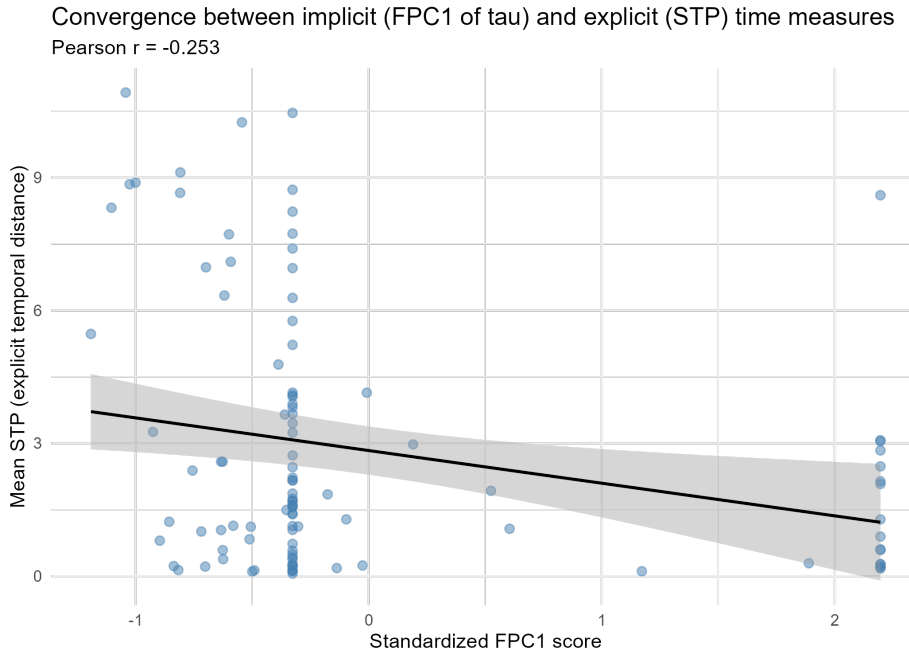


Figure 14: Scatterplot between the standardized first FPCA score of the centered subjective time trajectories and the individual mean STP measure. The fitted line provides a visual summary of the association between implicit and explicit subjective time measures.

Figure 15 reports the descriptive distributions of age, the Temporal Sense Scale, financial literacy, and the individual discount rate  $k_i$  by functional cluster.

Figures 16–20 report supplementary robustness checks for the functional clustering solution. The checks evaluate whether the three-cluster structure depends on the number of FPCs used for clustering, the clustering algorithm, the choice of distance or semi-metric, and the number of spline bases used in the smoothing steps. The Adjusted Rand Index is used to compare each alternative solution with the reference partition obtained from the first two standardized FPCA scores. Figure 16 shows that the reference partition is unchanged when three or four FPCs are used instead of two. When five or six FPCs are included, the Adjusted Rand Index remains above 0.80, although the average silhouette decreases. This result supports the use of the first two FPCs, which already explain 97.44% of the variability of the centered subjective time trajectories.

Figure 17 reports the robustness of the partition to alternative clustering specifications. The same partition is recovered across several  $k$ -means specifications and through PAM applied to the FPCA-score distance, whereas Ward.D2 produces a highly similar solution. This indicates that the clustering structure is not an artefact of a specific  $k$ -means implementation.

Figure 18 compares the reference partition with solutions obtained from alternative functional distances and derivative-based semi-metrics. The  $L^2$  distance on centered subjective

Cluster profiling: demographic and psychometric variables  
k = 3 functional clusters of tau(t)

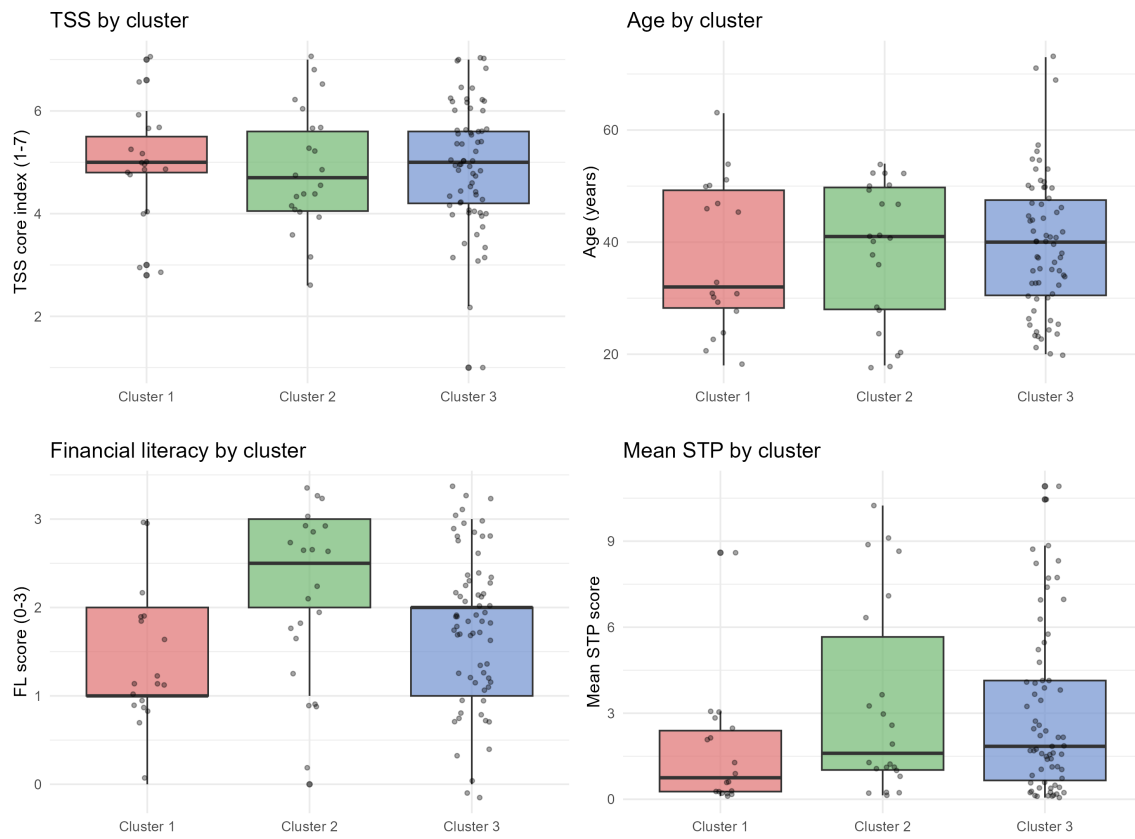


Figure 15: Descriptive distributions of age, TSS core index, financial literacy, and the individual discount rate  $k_i$  by functional cluster.

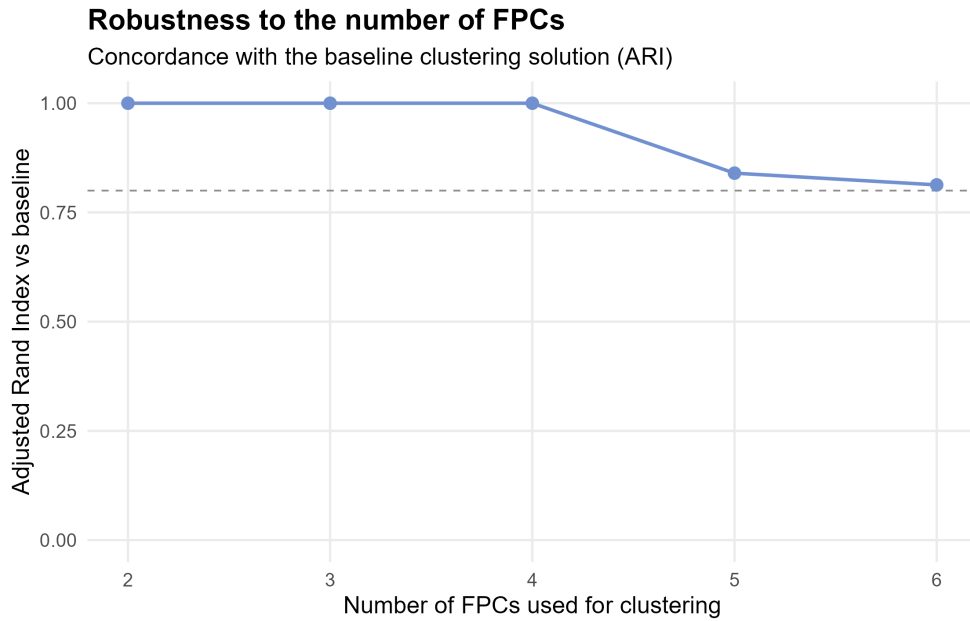


Figure 16: Robustness of the clustering solution with respect to the number of FPCs used for clustering. The Adjusted Rand Index compares each alternative partition with the reference solution based on the first two standardized FPCA scores.

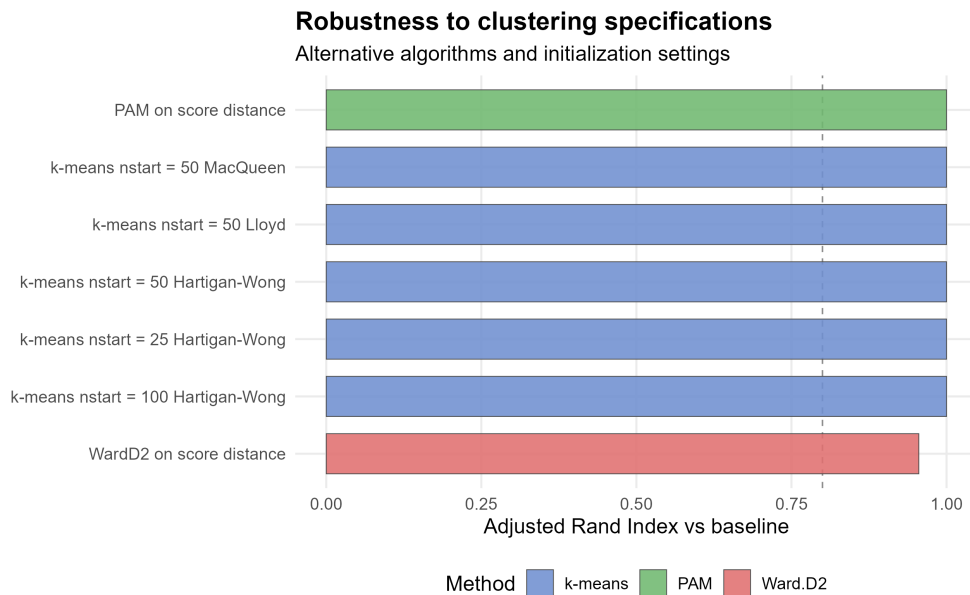


Figure 17: Robustness of the three-cluster solution under alternative clustering specifications. Values close to one indicate high agreement with the reference partition.

time trajectories leads to partitions highly consistent with the FPCA-score solution. In contrast, derivative-based semi-metrics yield lower agreement, especially for the second derivative. This result does not invalidate the reference clustering, but indicates that clustering on levels and clustering on local dynamic features emphasize different aspects of subjective time deformation.

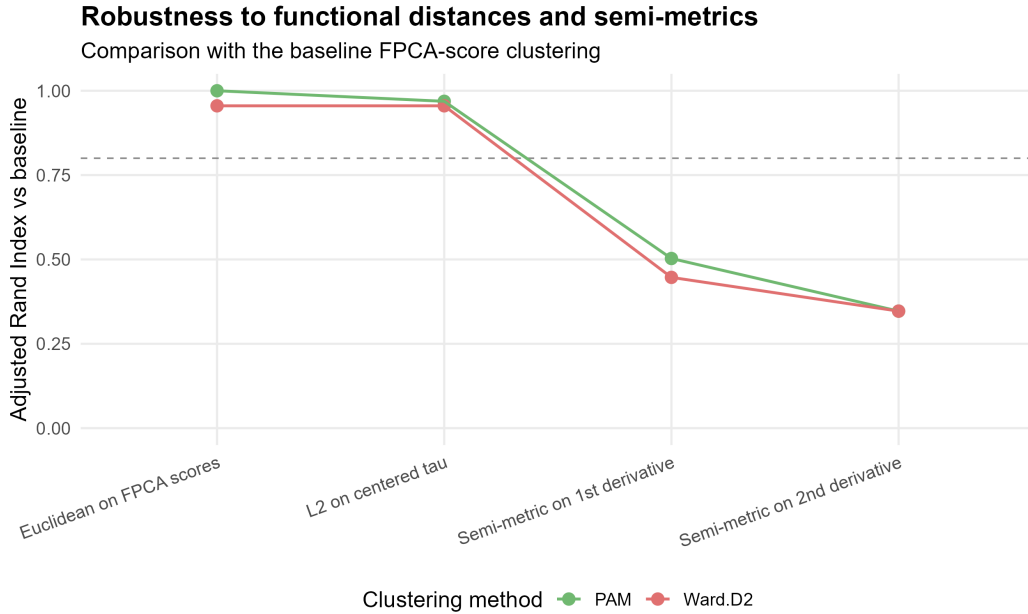


Figure 18: Robustness of the clustering solution under alternative functional distances and derivative-based semi-metrics. Lower agreement for derivative-based semi-metrics indicates that local dynamic features capture complementary information relative to the centered trajectories.

Figure 19 reports the sensitivity analysis with respect to the number of spline bases used in the monotone smoothing of  $f_i(t)$  and  $\tau_i(t)$ . Across the nine considered combinations, the Adjusted Rand Index with respect to the reference solution is always equal to 0.969 or 1. The proportion of variance explained by the first FPC remains between 0.803 and 0.823, while the cumulative variance explained by the first two FPCs remains between 0.974 and 0.992. These results indicate that the main FPCA and clustering structure is not driven by a specific smoothing-basis choice.

Figure 20 summarizes all robustness checks. Out of 29 alternative specifications, 25 yield an Adjusted Rand Index greater than or equal to 0.80, and the median Adjusted Rand Index equals 1. This provides supplementary evidence that the main clustering structure is stable with respect to several methodological choices.

### Sensitivity to smoothing bases (heatmap)

ARI compared with the baseline basis configuration

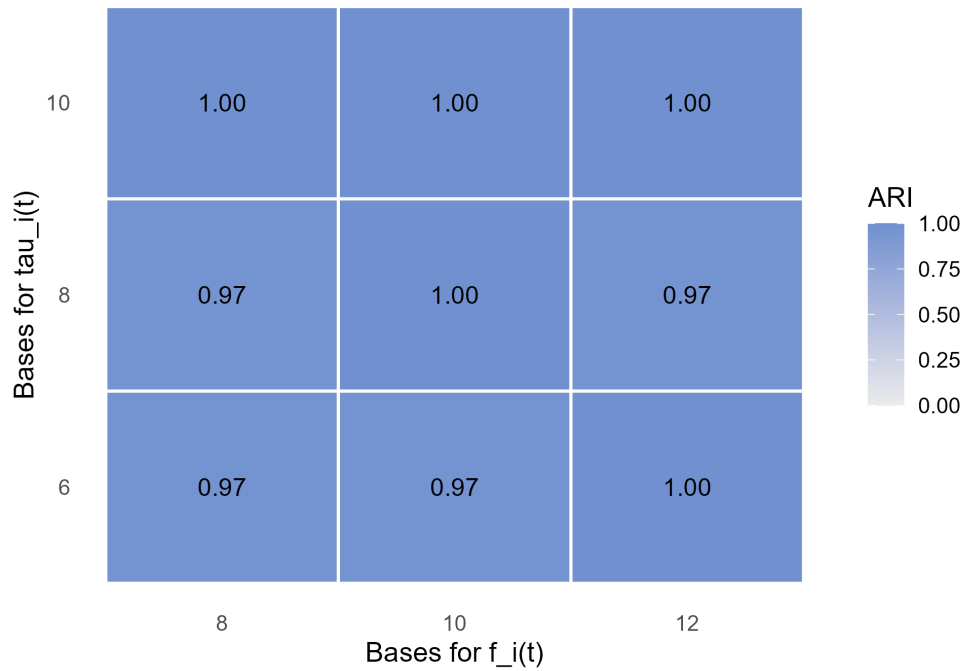


Figure 19: Sensitivity of the clustering solution to alternative smoothing-basis specifications for  $f_i(t)$  and  $\tau_i(t)$ . Each cell reports the Adjusted Rand Index relative to the reference solution.

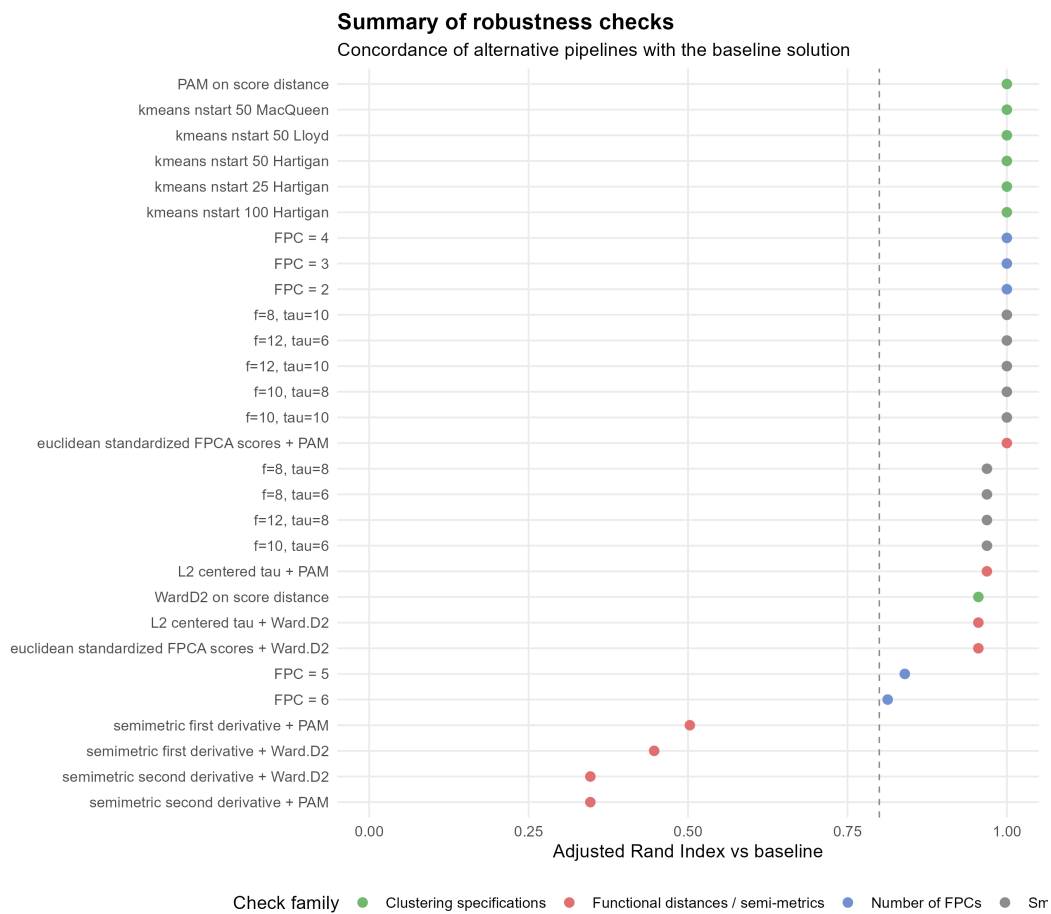


Figure 20: Summary of robustness checks. The figure reports the Adjusted Rand Index between each alternative solution and the reference clustering partition.